Basin and Petroleum System Modeling
8th Annual Industrial Affiliates Meeting
and
Field Trip to Salinas Basin

November 3-5, 2015
Stanford, California

Meeting Guide compiled by Allegra Hosford Scheirer and Jane Moss
Field Trip Guide by Tess Menotti and Steve Graham
http://bpsm.stanford.edu

2015 BPSM Industrial Affiliates

California Resources Corporation
Chevron
ConocoPhillips
Ecopetrol (new for 2016!)
Hess Corporation
Murphy Exploration & Production Co
Nexen Petroleum Inc.
PEMEX (new for 2015!)
Petrobras
Saudi Aramco
Southwestern Energy (new for 2015!)
with special thanks to
Schlumberger

Schedule of Events

Tuesday, 11/3/15, 5:30-7:30 p.m.	Icebreaker at Stanford Golf Course
Wednesday, 11/4/15, 7:30 a.m.-5:30 p.m.	Field Trip to Salinas Basin
Thursday, 11/5/15, 9 a.m.-5 p.m.	Oral Session at Stanford's Black Community Services Center
Thursday, 11/5/15, 6 p.m.	Il Fornaio Restaurant, 520 Cowper St, Palo Alto

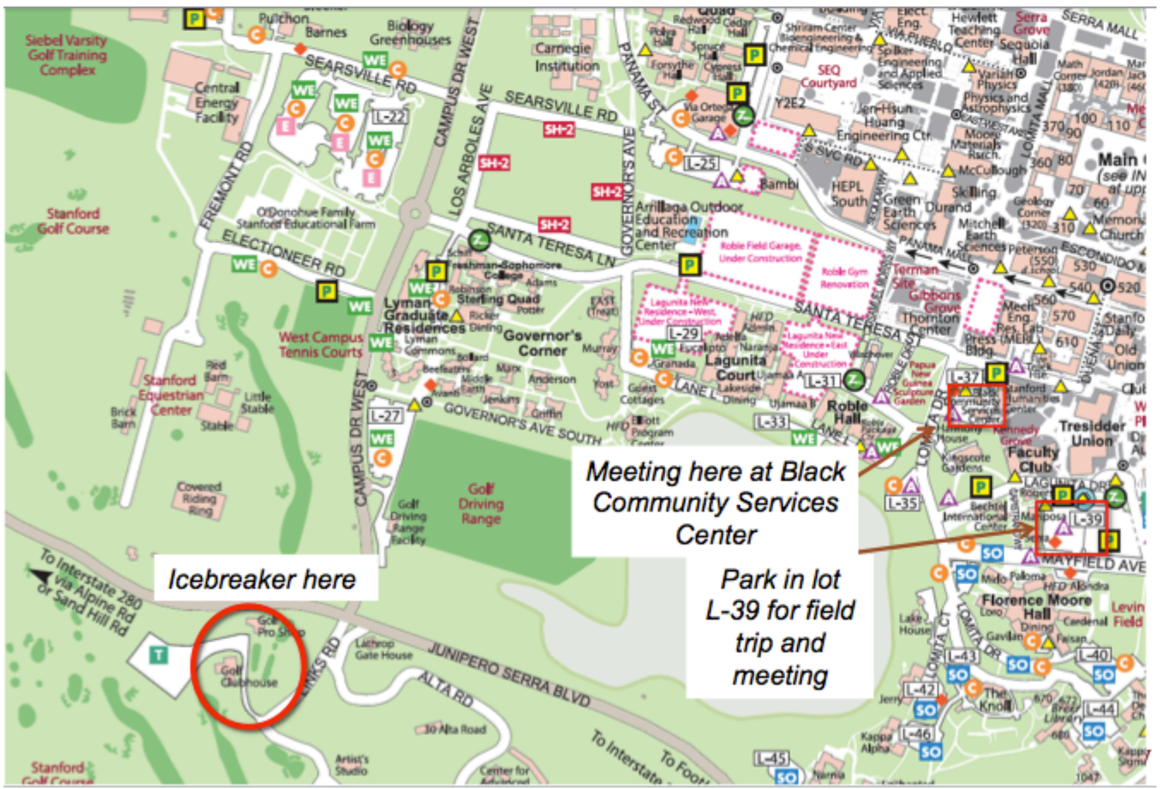

Parking is reserved for Wednesday and Thursday in lot L-39.

November 5, 2015 Oral Session Agenda

9:00 a.m.	**Steve Graham**, Introduction
9:20 a.m.	**Devon A. Orme**, Assessing Controls on Forearc Basin Subsidence: A 3D Subsidence Analysis of the Great Valley Forearc, California
9:45 a.m.	**Lauren Schultz**, Evaluating the Thermal History of the Los Angeles Basin Through 3d Basin and Petroleum System Modeling
10:10-10:25 a.m.	**Coffee break**
10:25 a.m.	**Inessa Yurchenko**, Shublik Shale Resource System: New Insights and Implications for Arctic Alaska Resource Potential
11:15 a.m.	**Will Thompson-Butler**, Colombia's Middle Magdalena Valley: Geologic Background and 1D Basin and Petroleum System Modeling
11:40 a.m.	**Laainam (Best) Chaipornkaew**, Introduction
11:50 a.m.	**Zack Burton**, Characterizing the Exhumation Path of the First Ultrahigh-Pressure Terrane in North America
12:15-1:30 p.m.	**Lunch** on the patio
1:30 p.m.	**Mustafa Al Ibrahim**, Stochastic Multiscale Electrofacies Classification of Well Logs as a Prelude to High-Resolution Basin and Petroleum System Modeling
1:55 p.m.	**Yao Tong**, 3D Basin and Petroleum System Modeling for the Piceance Basin and Source Rock Maturation History
2:30 p.m.	**Jens-Erik Lund Snee**, Predicting Overpressure Using Basin Modeling Software
3:00 - 3:15 p.m.	**Coffee break**
3:15 p.m.	**Wisam AlKawai**, The Impact of Allochthonous Salt Evolution and Overpressure Development on the Petroleum System in Thunder Horse Mini-Basin
4:05 p.m.	**Yao Tong**, Constraining Basin Thermal History and Petroleum Generation Using Paleoclimate Data in the Piceance Basin, Colorado
4:25 p.m.	**Ken Peters**, Upcoming events in 2016
4:30 p.m.	**Tapan Mukerji**, Value of information in Earth Sciences

2015 Meeting Attendees

Attendee	Organization
Timothy Boyler	California Resources Corp.
Alan Burnham	Consulting Prof., Stanford University
Kim Butler	Southwestern Energy Company
Blair Chan	ConocoPhillips
Gretchen Gillis	Aramco Services Company
John Guthrie	Hess Corporation
Mike Moldowan	Biomarker Technologies, Inc. (SU Emeritus)
Benjamin Kirkland	Nexen Petroleum
Julianne Lamb	Southwestern Energy Company
Rodrigo Maldonado Villalon	PEMEX
Guillermo Mora Oropeza	PEMEX
Fausto Mosca	Murphy Exploration & Production Company
Gary Muscio	Chevron
Ken Peters	Schlumberger (also at Stanford)
Tom Pinault	California Resources Corp.
Noelle Schoellkopf	Schlumberger (also at Stanford)
Christopher Sine	California Resources Corp.

BPSM Scientists	
Mustafa Al Ibrahim	Graduate Student
Wisam AlKawai	Graduate Student
Zachary Burton	Graduate Student
Laainam (Best) Chaipornkaew	Graduate Student
Steve Graham	Co-Principal
Allegra Hosford Scheirer	Co-Principal
Jens-Erik Lund Snee	Graduate Student
Les Magoon	Co-Principal
Tapan Mukerji	Co-Principal
Devon Orme	Post-doctoral Scholar
Lauren Schultz	Graduate Student
Will Thompson-Butler	Graduate Student
Yao Tong	Graduate Student
Inessa Yurchenko	Graduate Student

2015 Meeting Abstracts

http://bpsm.stanford.edu

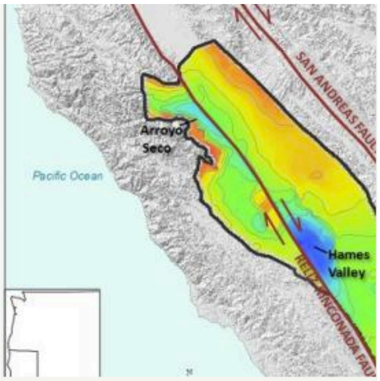

Salinas Basin, California

The Salinas basin is a Cenozoic strike-slip basin in the Coast Ranges of central California.

FAULTING STUDIES

SALINAS BASIN, CALIFORNIA

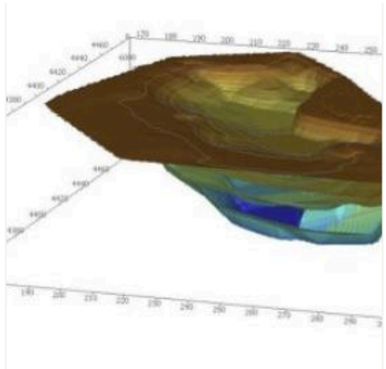

Piceance Basin, Colorado

The Piceance Basin is an asymmetrical sedimentary basin in the northeast part of the Colorado Plateau.

THEORETICAL STUDIES

PIECEANCE BASIN, COLORADO

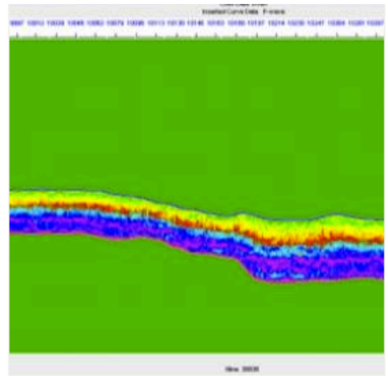

Gulf of Mexico

The study area in the Gulf of Mexico is located off the coast of Louisiana in the Ship Shoal and South Timbalier area.

PORE PRESSURE STUDIES

GULF OF MEXICO

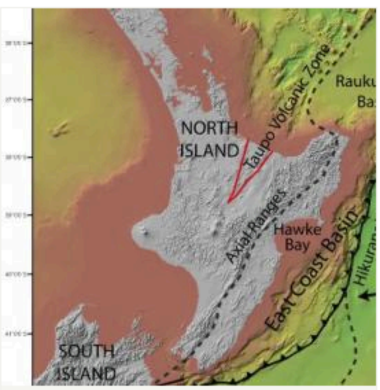

East Coast Basin, New Zealand

The East Coast Basin (ECB) is a petroliferous Neogene forearc basin located on the eastern margin on the North Island, New Zealand.

anford.edu/gulf-mexico

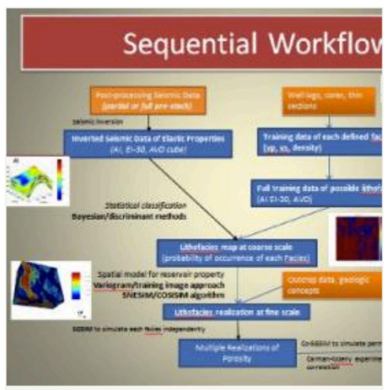

Understanding petrophysics of shale to calibrate regional basin models

Second-year Masters student Minh Tran works at the intersection of

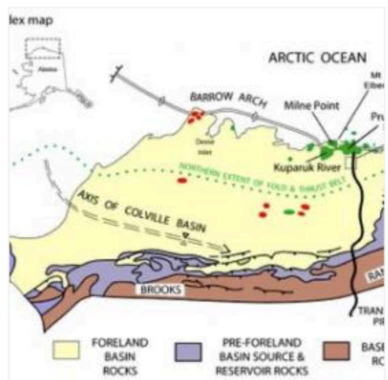

Source Rock Geochemistry, Stratigraphic Architecture, Unconventional Shale Resource Analysis and Petroleum System Modeling: Central North Slope

ASSESSING CONTROLS ON FOREARC BASIN SUBSIDENCE: A THREE-DIMENSIONAL SUBSIDENCE ANALYSIS OF THE GREAT VALLEY FOREARC, CALIFORNIA

Devon A. Orme, Steve Graham, Allegra Hosford Scheirer, and Les Magoon
Department of Geological Sciences, Stanford University

Forearc basins evolve between the magmatic arc and the accretionary prism of convergent margins and are important sediment archives detailing margin history. Forearc basins often contain several kilometers of sedimentary rocks and are characterized by high magnitude subsidence. However, unlike other types of basins, such as foreland or rift basins (DeCelles and Giles, 1996; McKenzie, 1978), the fundamental tectonic mechanisms controlling basin subsidence in a forearc basin are poorly understood (Xie and Heller, 2009; Angevine et al. 1990). Much of this challenge stems from the majority of modern forearcs being submarine, the investigation of which requires expensive deep-sea coring expeditions. Similarly, the majority are highly deformed and significantly eroded (e.g., Kázmér et al. 2003) or removed entirely by subduction erosion processes (Lallemand, 1998), although some ancient forearcs are preserved and subaerially exposed (e.g., Orme et al. 2014; Trop et al., 2008; Dürr, 1996; Garzanti and Van Haver, 1988). Thus, the majority of both ancient and modern forearc basins lack the necessary data for a thorough three-dimensional (3D) subsidence analysis necessary to produce a distinctive forearc tectonic subsidence curve.

The Great Valley forearc in California represents a notable exception to these limitations because it preserves an impressive succession of basin deposits that detail the processes active during its development, and thus provides a rare opportunity to study the life cycle of a forearc basin. Extending for 680 km along the continental margin, the Great Valley forearc was part of a series of forearc basins that developed from Early Cretaceous to early Cenozoic time as oceanic crust subducted beneath the western margin of North America (Dickinson, 1995; Ingersoll, 1976). The Great Valley forearc was part of an accretionary forearc system (e.g., Clift and Vannucchi, 2004) that developed between the Franciscan subduction complex to the west and the Sierra Nevada magmatic arc to the east (Figure 1). Unlike other ancient convergent margins, such as the Mesozoic Andean margin, drastic changes in the geometry of the subducting plate (e.g., subduction angle) along western North America did not cause the magmatic arc and forearc system to migrate substantially thorough time. Thus, a thick stratigraphic succession more than 13 km was deposited during the Mesozoic and early Cenozoic (Ingersoll, 1976). Following a change from convergence to transform motion along the California margin in the Oligocene, the central part of the Great Valley forearc basin was preserved as the San Andreas Fault developed in place of the subduction trench.

The preservation of the Great Valley forearc has led to over 60 years of research devoted to understanding its evolution. Much of this study focuses as well on deep-water sedimentological processes that contributed to the development of vast petroleum and natural gas reservoirs within the forearc basin succession (Graham, 1987). Recent advances in detrital zircon geochronology and provenance analysis have led to new models of sediment dispersal patterns, which link changes in the geometry of the subducting slab in the Late Cretaceous to changes in sedimentation in the Great Valley forearc (Sharman et al. 2015; Dumitru et al. 2010; DeGraff-Surpless et al. 2002). In addition, the availability of high quality proprietary 2D and 3D seismic reflection surveys has enabled subsurface analysis of the stratigraphic architecture of the basin. Despite these efforts, much of the subsidence history of the Great Valley forearc remains poorly understood. Aside from some notable exceptions (Williams and Graham, 2013; Williams, 1997; Moxon, 1988), most studies conducted thus far have placed little emphasis on deciphering the tectonic component of basin subsidence.

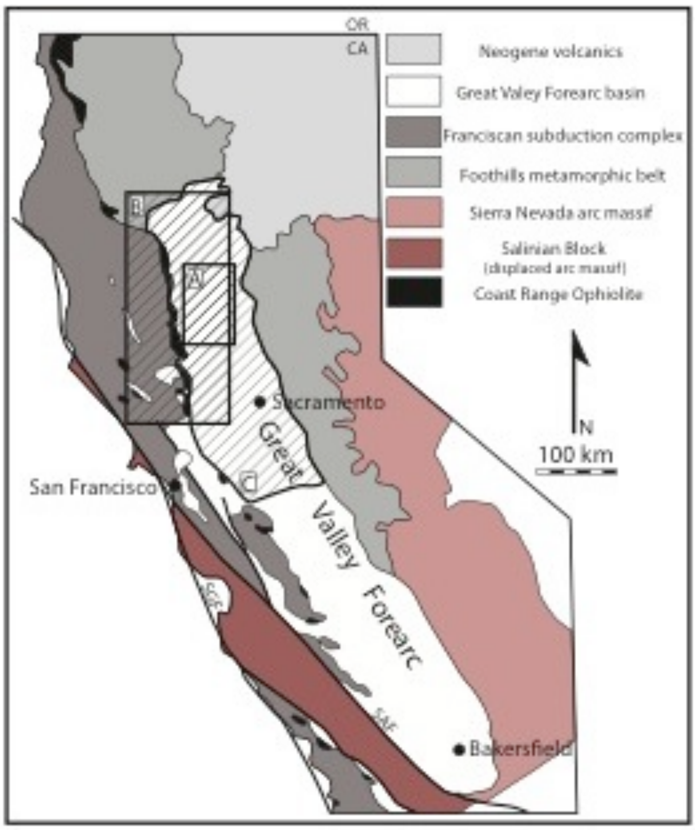

Figure 1. Generalized geologic map and locations of data to be used in this study (after Williams and Graham, 2013; Ingersoll, 1988; and Dickinson et al., 1979. SAF: San Andreas Fault; SGF: San Gregorio-Hosgri Fault.

This study thus seeks to define a holistic model for forearc basin evolution by performing the first 3D tectonic subsidence analysis of the well-preserved Mesozoic–early Cenozoic Great Valley forearc basin in central-northern California using previously proprietary seismic and borehole data (Figure 1). Geologic information, including spatial-temporal facies distributions, paleowater depth, and erosion estimates evidenced by basin unconformities will be combined with horizon depth maps and other seismic and well information to build a 3D model for the Sacramento Basin. The objectives of this study are to *(1) quantify the spatial patterns, timing and rates of subsidence in the Great Valley forearc and (2) use these results to define a framework for interpreting subsidence trends in other ancient and modern forearc basins*. It is hypothesized herein that the shape of a forearc tectonic subsidence curve may be predicted and used to understand spatial and temporal processes driving subsidence in forearc basins worldwide, provided that detailed 2D and 3D seismic data and ample borehole data are available. The results of this study have broader implications for understanding and explaining the evolution of the Californian margin and accretionary convergent margins in other regions. This work will also serve as the basis for future modeling of the petroleum systems within the Great Valley forearc.

References

Angevine, C.L., Heller, P.L., and Paola, C., 1990, Quantitative sedimentary basin modeling: American Association of Petroleum Geologists Short course Note Series, 32, 247 pp.
Clift, P.D. and Vannucchi, P., 2004, Controls on tectonic accretion versus erosion in subduction zones: Implications for the origin and recycling of the continental crust. *Rev. Geophys*, 42, RG2001.

DeCelles, P.G., and Giles, K.A., 1996, Foreland basin systems, *Basin Research*, 8, 105–123.

DeGraaff-Surpless, K., Graham, S.A., Wooden, J.L., and McWilliams, M.O., 2002, Detrital zircon provenance analysis of the Great Valley Group, California: Evolution of an arc-forearc system, *Geological Society of America Bulletin*, 114(12), 1564–1580.

Dickinson, W.R., 1995, Forearc basins, *in* Busby, C.J., and Ingersoll, R.V., eds., Tectonics of sedimentary basins: Cambridge, Massachusetts, Blackwell Science, 221–261.

Dürr, S.B., 1996, Provenance of Xigaze forearc basin clastic rocks (Cretaceous, south Tibet): *Geological Society of America Bulletin*, 108, 669-684.

Dumitru, T.A., Ernst, W.G., Wright, J.E., Wooden, J.L., Wells, R.E., Farmer, L.P., Kent, A.J.R, and Graham, S.A., 2013, Eocene extension in Idaho generated massive sediment floods into the Franciscan trench and into the Tyee, Great Valley, and Green River basins: Geology, v. 41, p. 187-190, doi: 10.1130/G33746.1.

Garzanti, E. and Van Haver, T., 1988, The Indus clastics: Forearc basin sedimentation in the Ladakh Himalaya (India), *Sedimentary Geology,* 59(3-4), 237-249.

Graham, S.A., 1987, Tectonic controls on petroleum occurrence in central California, *in* Ingersoll, R.V., and Ernst, W.G., eds., Cenozoic basin development

Ingersoll, R.V., 1976, Evolution of the Late Cretaceous forearc basin of northern and central California, Ph.D. dissertation: Stanford University, 200 p.

McKenzie, D.P., 1978, Some remarks on the development of sedimentary basins, *Earth and Planetary Science Letters*, 40 (1), 25-31.

Xie, X., and Heller, P., 2009, Plate tectonics and basin subsidence history, *Geological Society of America Bulletin*, 121, 55–64.

Kázmér, M., Dunkl, I., Frisch, W., Kuhlemann, J., Ozsvárt, P., 2003, The Palaeogene forearc basin of the Eastern Alps and Western Carpathians: subduction erosion and basin evolution, *Journal of the Geological Society of London,* 160, 413-428.

Moxon, I.A., Stratigraphic and Structural architecture of the San Joaquin and Sacramento Valleys, PhD dissertation: Stanford University, 371 p.

Orme, D.A., Carrapa, B., Kapp, P., 2014, Sedimentology, provenance, and geochronology of the Upper Cretaceous-Lower Eocene Western Xigaze forearc basin, southern Tibet, *Basin Research,* 27(4), 387-411.

Sharman, G.R., Graham, S.A., Grove, M., Kimbrough, D.L., Wright, J.E., 2015, Detrital zircon provenance of the late Cretaceous-Eocene California forearc: Influence of Laramide low-angle subduction on sediment dispersal and paleogeography, *Geological Society of America Bulletin,* doi:10.1130/B31065.1.

Trop, J.M., 2008, Latest Cretaceous forearc basin development along an accretionary convergent margin: South-central Alaska, *Geological Society of America Bulletin*, 120(1-2), 207–224.

Williams, T.A. and Graham, S.A., 2013, Controls on forearc basin architecture from seismic and sequence stratigraphy of the Upper Cretaceous Great Valley Group, central Sacramento Basin, California, *International Geology Review,* 55(16), 2030-2059.

Williams, T.A., 1997, Basin-fill architecture and forearc tectonics, Cretaceous Great Valley Group, Sacramento basin, northern California, Ph.D. thesis, Stanford University, 412 pp.

EVALUATING THE THERMAL HISTORY OF THE LOS ANGELES BASIN THROUGH 3D BASIN AND PETROLEUM SYSTEM MODELING

Lauren E. Schultz[1], Allegra Hosford Scheirer[1], Ken Peters[1,2], Tom Wright[3], and Stephan A. Graham[1]
[1]*Department of Geological Sciences, Stanford University*
[2]*Schlumberger Information Solutions*
[3]*Geologist*

The Los Angeles Basin presents a valuable opportunity for 3D basin and petroleum system modeling due to its impressively high hydrocarbon productivity relative to sediment volume, high source rock total organic carbon, and the geochemical diversity of the produced oils. A 3D Earth model of the Los Angeles Basin was constructed from basement to ground surface to examine the various factors impacting heat flow through the basin's history. The basement surface is defined by the Southern California Earthquake Center (SCEC) Community Velocity Model, and supplemented by well penetrations on the basin flanks. Overlying sedimentary strata are mapped from well logs, to include top Pico, Repetto and Monterey (Puente) formations, as well as several chronostratigraphic surfaces, including top Miocene, Oligocene, Eocene and Paleocene. The Miocene Puente Formation is additionally subdivided into several subunits, including the organic-rich Nodular Shale source rock unit (Figures 1 and 2).

The chief aim of this model is to better understand the impacts of the basin's complex geologic history on the thermal history of the basin. The relative impacts and magnitudes of the various thermal effects are explored from a basin modeling perspective through scenario testing and comparison with calibration data and mapped source rock maturity trends, buttressed by new custom bulk kinetics of the Nodular Shale phosphatic source rock. We examine the following successive tectonic episodes having conflicting thermal effects: a) pre-basinal subduction of the Farallon plate through the Paleogene resulting in early depression of isotherms b) subsequent subduction of the East Pacific Rise and transition to a transform plate boundary, associated with volcanism, schist upwelling and increased heat flow; and c) rapid subsidence of the basin initiated in the middle to late Miocene, producing in turn a cooling effect through the thermal blanketing effects of deposited sediments and the lateral heat loss through steep basin margins. This new model of the Los Angeles Basin will provide for a more comprehensive understanding of this basin's unique petroleum system.

Figure 1. Stratigraphy of the Los Angeles basin with source rocks, including the nodular shale and Puente/Monterey Fm, highlighted in yellow, and important reservoir rocks, including the Pico and Repetto Formations, highlighted in red. Modified from Beyer, 1995.

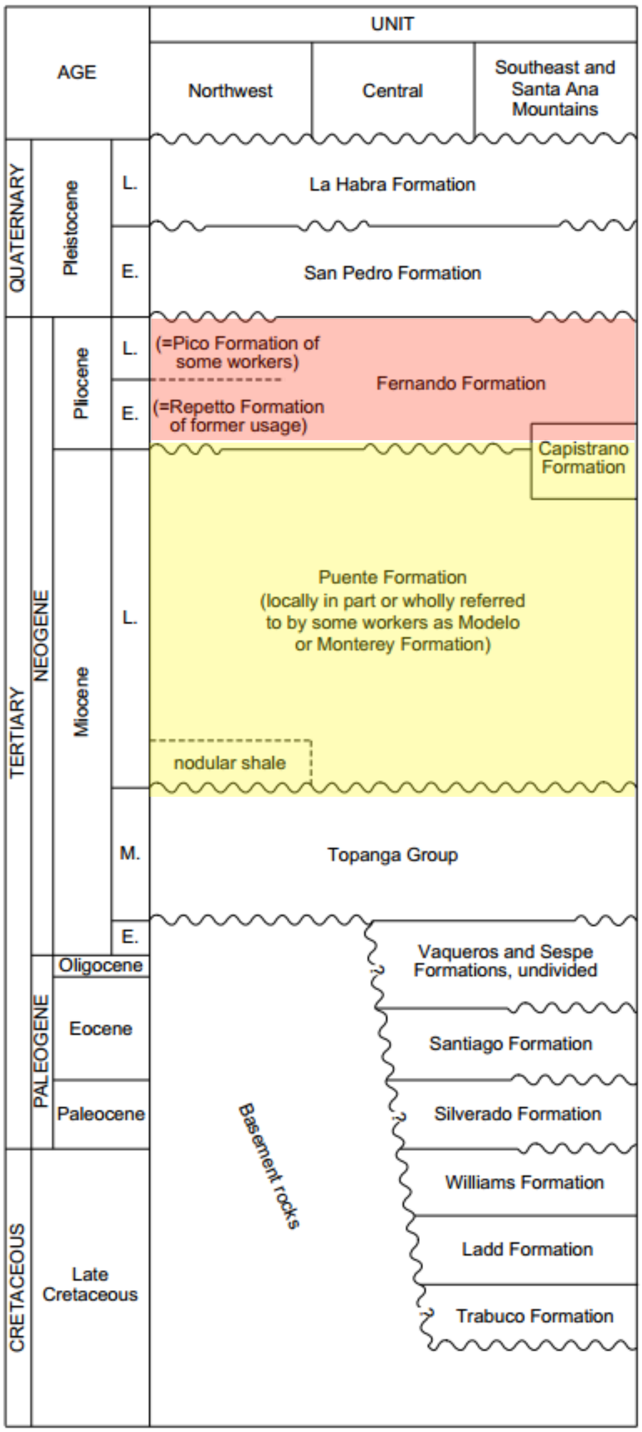

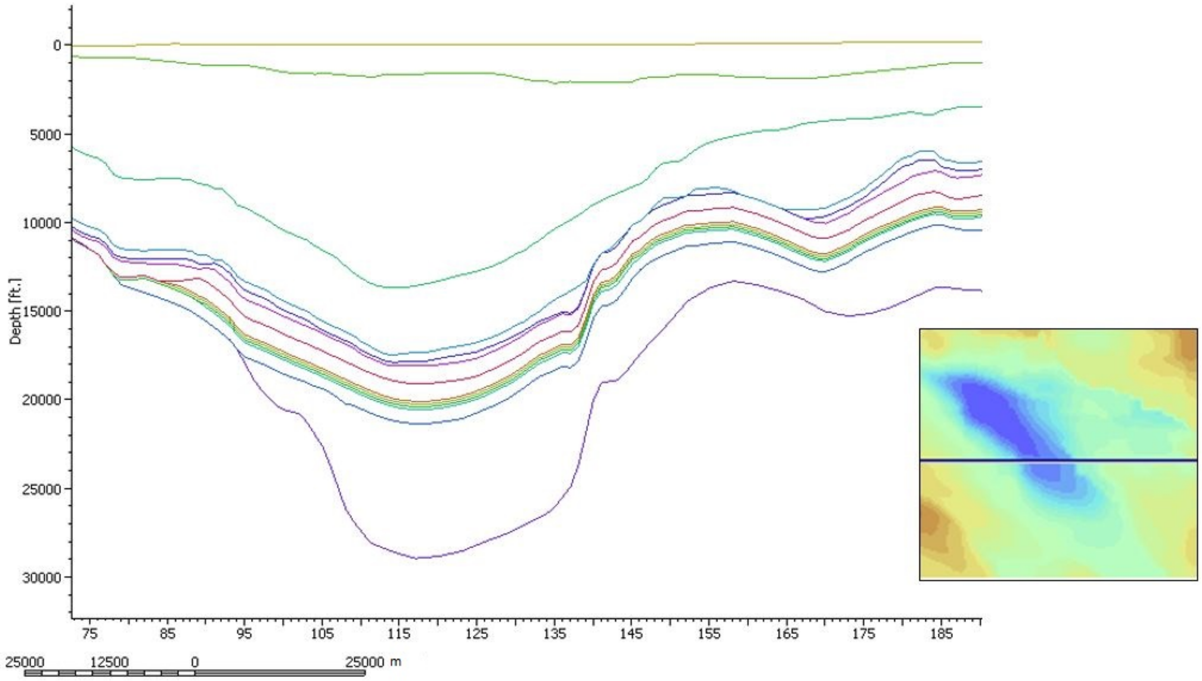

Figure 2. Cross-section of 3D model through the Los Angeles Basin central trough (inset) with the following chronostratigraphic surfaces (from base to top): basement, Cretaceous, Paleocene, Eocene, Oligocene, Lower Miocene, Middle Miocene, Lower Mohnian (source rock interval), Mohnian, Upper Miocene, Repetto Formation (reservoir rock interval), Pico Formation (reservoir rock interval), and present-day topography. Note the extreme depth of the basement surface.

SHUBLIK SHALE RESOURCE SYSTEM: NEW INSIGHTS AND IMPLICATIONS FOR ARCTIC ALASKA RESOURCE POTENTIAL

Inessa Yurchenko, Les Magoon, Allegra Hosford Scheirer, and Steve Graham
Department of Geological Sciences, Stanford University

Recent shale-oil and shale-gas exploration and production success has sparked scientific interest in the identification of new unconventional hydrocarbon reservoirs. In particular, much work has been done in understanding the distribution of source rock and source-rock-as-reservoir-rock properties in order to accurately assess resource potential (Jarvie, 2012). A shale resource system is described as an organic-rich mudstone(s) that serves as both source and reservoir rock for generated oil and gas (Jarvie, 2012). It can also charge and seal petroleum in juxtaposed organic-lean facies. Thus, all the elements and processes of a conventional petroleum system (Magoon and Dow, 1994) are applicable to these shale resource systems. The pod of active source rock is a particularly key component of these types of systems. However, due to significant spatial variability in lithology and quality, quantity and thermal maturity of organic matter within a source rock, it is important to recognize and quantify its geochemical and lithological heterogeneity.

Although it has been recognized that organic-rich sediments vary lithologically, the majority of source rock research is historically focused on detailed geochemical assessments rather than sedimentological analysis. Conventional cores are primarily drilled for reservoir rocks, and much of the source rock analysis has been done on cuttings and/or outcrop samples, creating interpretive pitfalls. Source rock coring is now an essential part of the unconventional shale resource exploration procedure, and it provides vast opportunities for advanced shale research.

Arctic Alaska is a prolific petroleum province that contains a great share of the US energy resources, however it still remains one of the least explored regions in the country (Bird, 2001). It has been widely recognized that crude oil accumulations in the North Slope commonly represent a mixture of oils derived from several source rocks, but the Middle to Upper Triassic Shublik Formation is considered to be the major source rock for oil in the North Slope and main contributor in the Prudhoe Bay field, the largest field in North America (Masterson, 2001, Peters et al., 2008). The Shublik Formation is a laterally and vertically heterogeneous unit that has been described both in outcrop and in the subsurface. Since Bailey (2012) proclaimed the Shublik as the main target of unconventional shale-oil exploration, understanding of its organic-rich facies distribution and petroleum potential has become of particular importance. Hutton et al. (2012) compared the Shublik Formation to the Cretaceous Eagle Ford Shale reservoir of South Texas. This work indicated some analogous attributes between the two, such as burial depth, thickness and total organic content, but also emphasized that further well control and reservoir characterization are necessary for successful resource exploitation (Hutton et al., 2012).

This research investigates source rock geochemistry, stratigraphic architecture, and unconventional shale resource analysis of the Shublik Formation in the context of petroleum system modeling. Organic geochemical studies involve source rock screening methods, analyses of biomarkers and diamondoids, including quantitative diamondoid analysis (QDA), quantitative extended diamondoid analysis (QEDA), and compound specific isotope analysis of diamondoids (CSIA-D). Advanced organic geochemical analyses were performed at Biomarker Technologies, Inc. Our goal is to determine if the chemostratigraphy of the Shublik Formation—determined through all these methods in combination with inorganic geochemical mapping—provides a basis for correlation between lithofacies, organofacies, and gamma ray patterns. If this turns out to be the case, stratigraphic architecture could be inferred through well-log correlations in the absence of extensive hard rock analyses.

In this talk, I will present preliminary results on core-to-core correlation using total organic carbon, carbonate content, and gamma ray patterns. Moreover, QEDA and complementary CSIA-D method results will be discussed and used for oil to source correlation (Fig. 1).

Further research will focus on incorporating knowledge of the Shublik Formation's heterogeneity and stratigraphic architecture in order to define source and reservoir rock intervals and to calculate the volume of hydrocarbons generated and still retained in the formation through a better understanding its hydrocarbon expulsion and storage capacity.

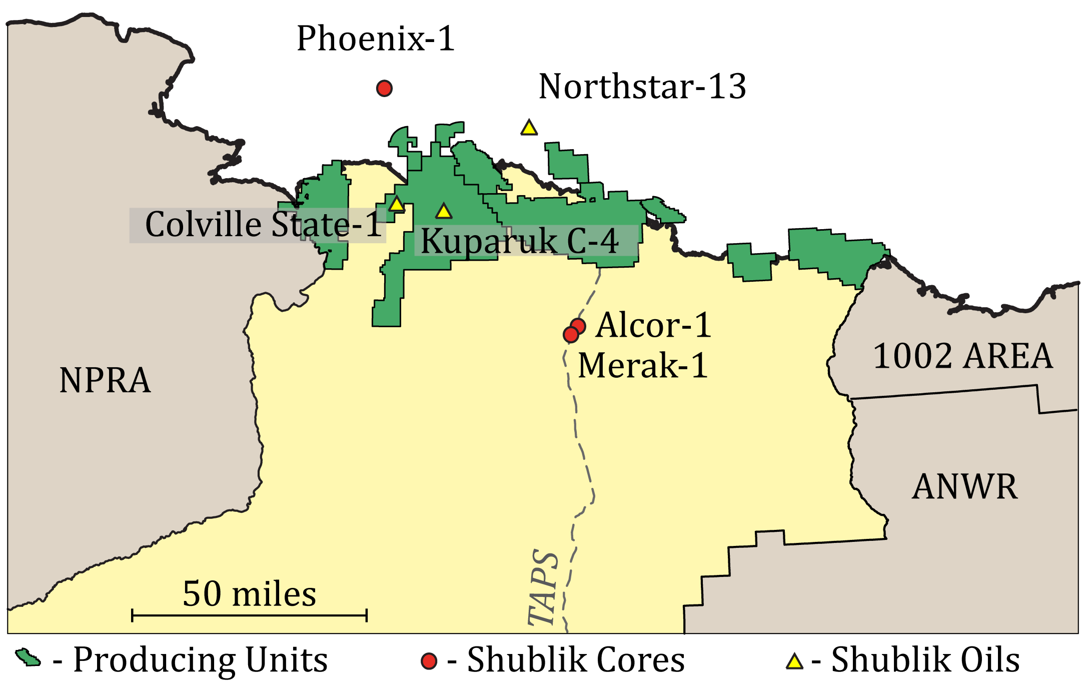

Figure 1. Map of a part of Arctic Alaska showing area of interest and key Shublik cores and oil samples locations. Central North Slope is indicated in yellow. NPRA - National Petroleum Reserve in Alaska, ANWR - Arctic National Wildlife Refuge.

References

Bailey, A., 2012, The oil's there: *Petroleum News*, 17, no. 39, 1–15.

Bird, K. J., 2001, Alaska: A twenty-first-century petroleum province, in M.W. Downey, J. C. Threet, and W. A. Morgan, eds., "Petroleum provinces of the twenty-first century", *AAPG Memoir 74*, p. 137-165.

Hutton, E., Agboada, D.K., Whalen, M.T., and Hanks, C.T., 2012, Upper Triassic Shublik Formation of North Alaska — An Eagle Ford Type Shale Reservoir Play?, *AAPG Search and Discovery Article* no. 10437.

Jarvie, D. M., 2012, Shale resource systems for oil and gas: Part 1—Shale-gas resource systems, in J. A. Breyer, ed., "Shale reservoirs - Giant resources for the 21st century", *AAPG Memoir* 97, p. 69–87.

Magoon, L. B. and W. G. Dow, 1994, "The petroleum system - from source to trap", *AAPG Memoir* 60.

Masterson, W. D., 2001, "Petroleum filling history of central Alaskan North Slope fields", *Ph.D. thesis, University of Texas at Dallas*, Dallas, Texas, 222 p.

Peters, K. E., Ramos, S. L., Zumberge, J. E., Valin, Z. C., and Bird, K. J., 2008, De-convoluting mixed crude oil in Prudhoe Bay Field, North Slope, Alaska, *Organic Geochemistry* 39.

COLOMBIA'S MIDDLE MAGDALENA VALLEY: GEOLOGIC BACKGROUND AND 1D BASIN AND PETROLEUM SYSTEM MODELING

Will Thompson-Butler, Les Magoon, and Steve Graham
Department of Geological Sciences, Stanford University

Abstract

In northwestern South America prolific Cretaceous-Tertiary petroleum systems exist and are actively produced. The La Luna source rock and equivalents alone have generated an estimated 2.3 trillion barrels of oil. As a result, vast reserves have accumulated regionally in sedimentary basins across Colombia, Venezuela, Trinidad, and Ecuador (Villamil et al, 2003). In Colombia, the Middle Magdalena Valley existed as a major sedimentary basin from the Triassic to the middle Miocene, during which time both the rich La Luna source rock and thick continental reservoir packages were deposited. With discoveries to date of about 2 billion barrels of oil and 3 trillion cubic feet of gas (ANH Colombian Sedimentary Basins report, 2007), the Middle Magdalena Valley remains an active exploration area. 1D Basin and Petroleum System modeling in the Middle Magdalena Valley illustrates the impact of the structural complexity in northwestern South America on the timing of petroleum generation as well as the potential for additional contributions from other Cretaceous source rocks. Further well and geohistory data are necessary to calibrate and improve the accuracy of the 1D models.

Geologic Background

The Colombian Andes are comprised of three NE-SW trending ranges, the Western, Central and Eastern Cordilleras, which merge to the south into a single range. The Magdalena Valley separates the Central and Eastern Cordilleras with the Middle Magdalena Valley (MMV) beginning north of Bogota (Figure 1).

Several tectonic events contributed to petroleum systems in the MMV. In the Triassic, Jurassic and earliest Cretaceous, rifting associated with the separation of N. and S. America in the proto-Caribbean resulted in the formation of two depocenters, the Tablazo-Magdalena and Cocuy basins, separated by the intrabasinal Santander high (Figure 2a). Contributing to basinal subsidence was back arc stretching related to the subduction zone off the western coast of Colombia. As a result of extension, deposition in the Tablazo-Magdalena basin was entirely marine until the late Cretaceous when deformation from the final accretion of the Western Cordillera created an early foreland basin in the MMV area (Figure 2b). As a result, deposition shifted from the rich marine source rocks of the early-late Cretaceous to more continental deposits.

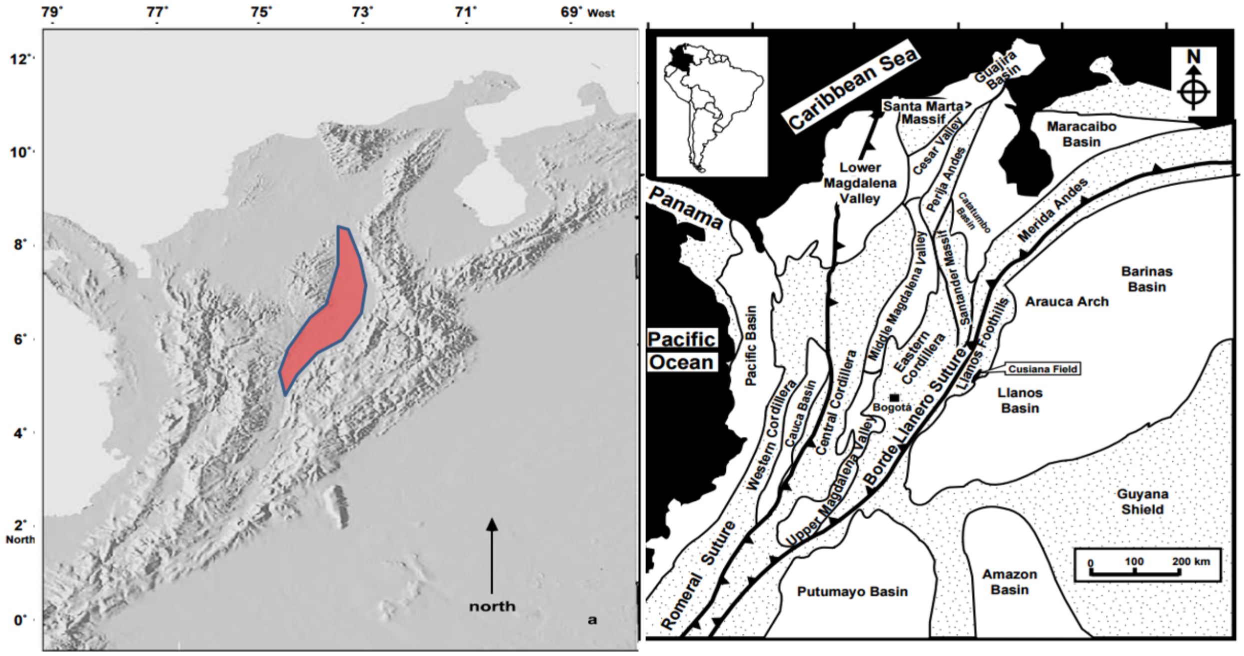

Figure 1. Maps of Colombia illustrating the location of the intermontane Middle Magdalena Valley in the context of the Western, Central and Eastern Cordilleras, as well as the other primary Colombian depocenters. Modified from figures by Cooper et al (1995) and Villamil (2003).

Major deformation and uplift of the Eastern Cordillera didn't begin until the Turtonian and resulted from the collision of Panama with South America. During this deformational period the Eastern Cordillera was uplifted and eroded. In the Middle Magdalena Valley, older extensional faults were inverted, new compressional faults formed, and folds from the middle Eocene were reactivated (Figure 2C). Of importance, deposition related to this late Neogene molasse finally pushed the middle-late Cretaceous source rock package into the oil window. A stratigraphic column for the MMV illustrating the relative timing of these primary tectonic events alongside the corresponding depositional units and petroleum system elements is shown in figure 3 (Cooper et al, 1995).

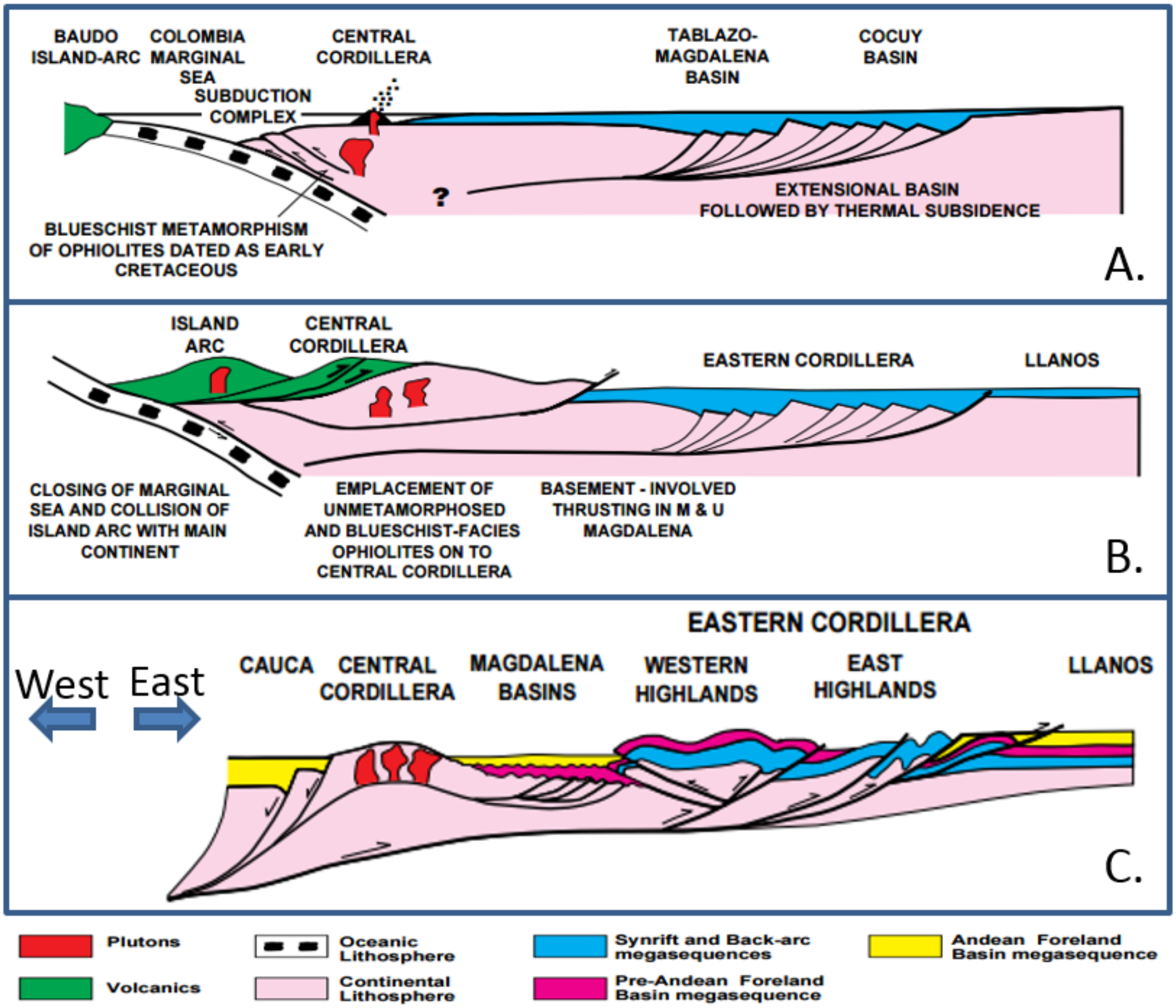

Figure 2. A schematic West-East cross-section from the Central Cordillera across the Middle Magdalena Valley, Eastern Cordillera, and Llanos illustrating the primary deformational regimes in NW South America. A.) Jurassic-Early Cretaceous Sequence following extension and subsidence. B.) Maastrichtian-Paleocene accretion of western cordillera and early foreland basin. C.) Middle Miocene-Recent Andean foreland basin. Modified from a figure by Cooper et al. (1995).

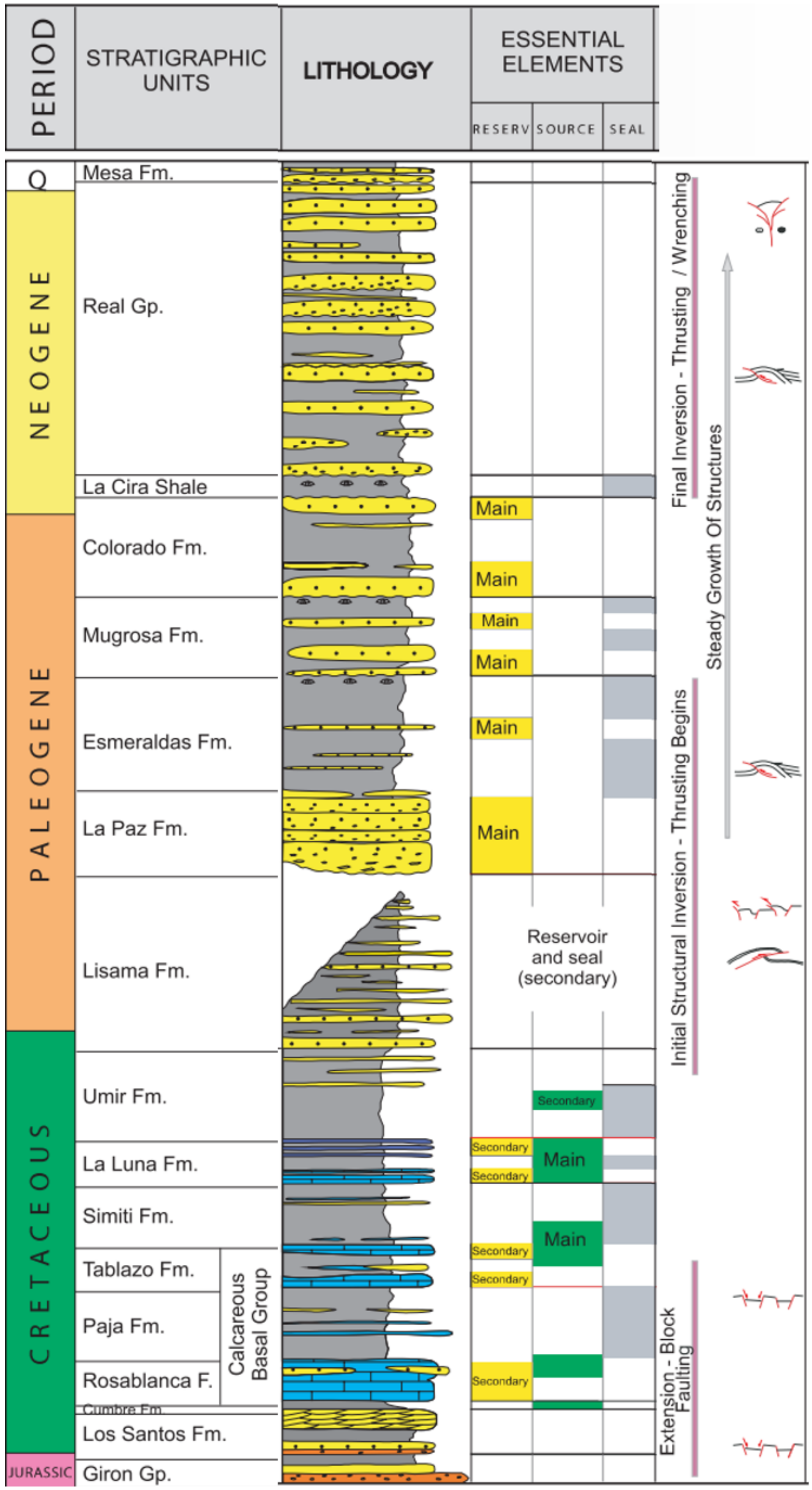

Figure 3. A stratigraphic column for the Middle Magdalena Valley illustrating the relative timing of the

primary tectonic events alongside the corresponding depositional units and petroleum system elements. Modified from ANH Colombian Sedimentary Basins report, 2007.

1D Middle Magdalena Valley Model

After compiling data for formation tops, custom lithologies, and basin history, enough information was available for preliminary 1D basin modeling. The Infantas 1613 well was selected for its central location in the MMV. The availability of vitrinite reflectance data in this well guided estimations of eroded thickness during compressional events and basal heat flow through time. A 1D model for the Infantas 1613 well that honors the thermal maturity indicators is shown in Figure 4a. The calculated burial history diagram for this well, overlain with predicted vitrinite reflectance for potential source rock units (Figure 4b), provides several key observations:

- The prolific La Luna formation, as predicted in the literature, remains in the early oil window.
- The compressional regimes and ensuing periods of erosion have delayed maturation of other Cretaceous source rock units to the extent that multiple petroleum systems may be active in the current day.
- The Rosa Blanca, a potential secondary source, is currently in the gas window. This unit left the oil window prior to Turtonian major deformation in the Eastern Cordillera. Many of the previous structural trapping configurations in the MMV may have been altered and new structural traps formed during this period. Accumulation and preservation would therefore be high-risk elements for a Rosa Blanca sourced petroleum system.
- The Tablazo Unit, also a potential secondary source, is currently in the late oil window and has been throughout the late Neogene. Tablazo co-sourced accumulations could be found in the MMV fields.

A second model was constructed for the Casabe 199 well located~20 km away. We used similar eroded thickness, lithologies, basin history information, and boundary conditions in this well as for the Infantas 1613 well. However, the calculated vitrinite reflectance differs from observed data at depth (Figure 5). With high uncertainty in basal heat flow, eroded thickness and other parameters, more data is required to refine these preliminary models. As a next step, building modeled surfaces from formation tops and acquiring more vitrinite reflectance data with broader coverage in the MMV will allow more accurate prediction of erosion thickness and basal heat flow over time.

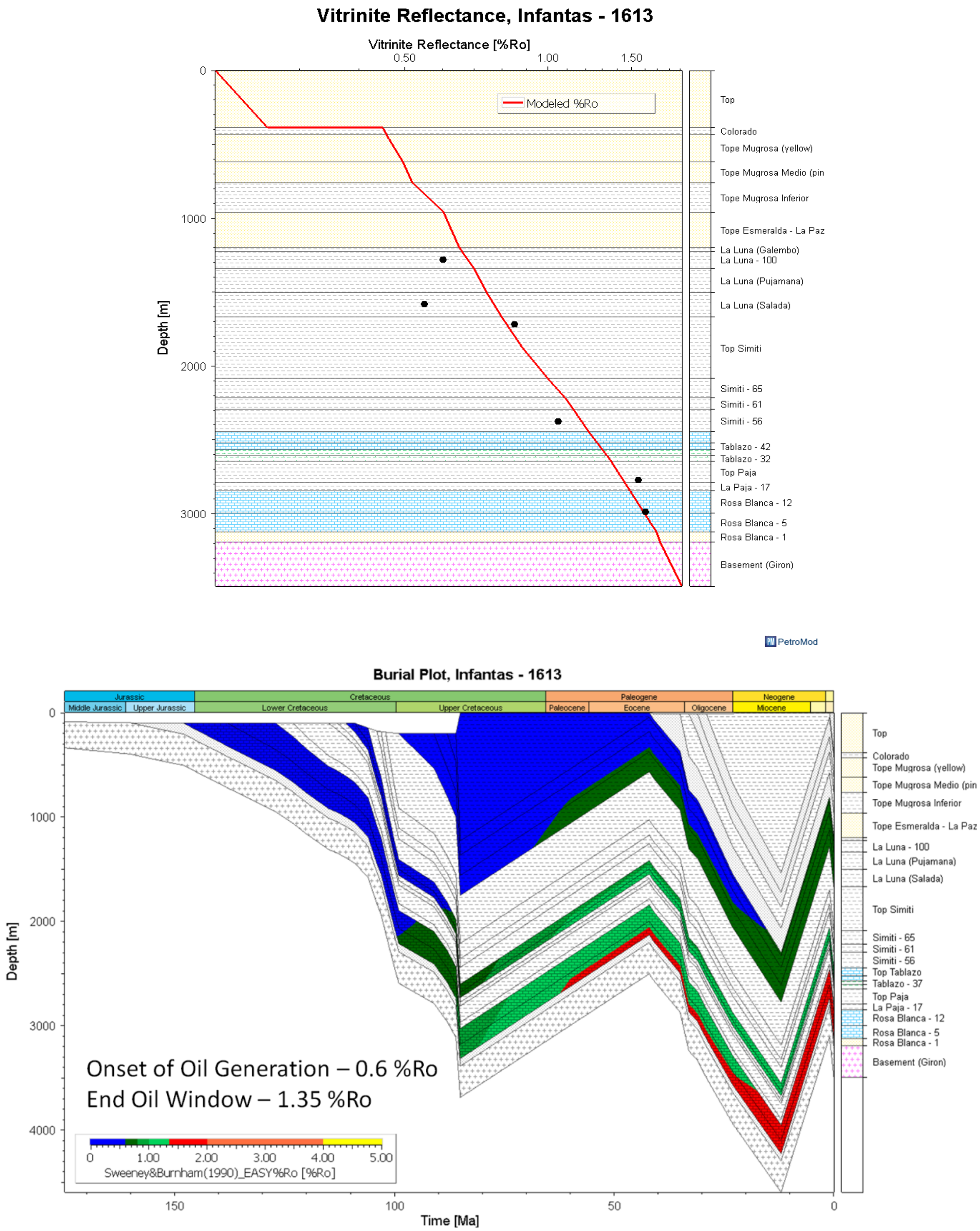

Figure 4. A.) Predicted and observed vitrinite reflectance (%R_o) for the Infantas 1613 well. B.) Burial history for this well shown with %R_o overlay on all source rock units.

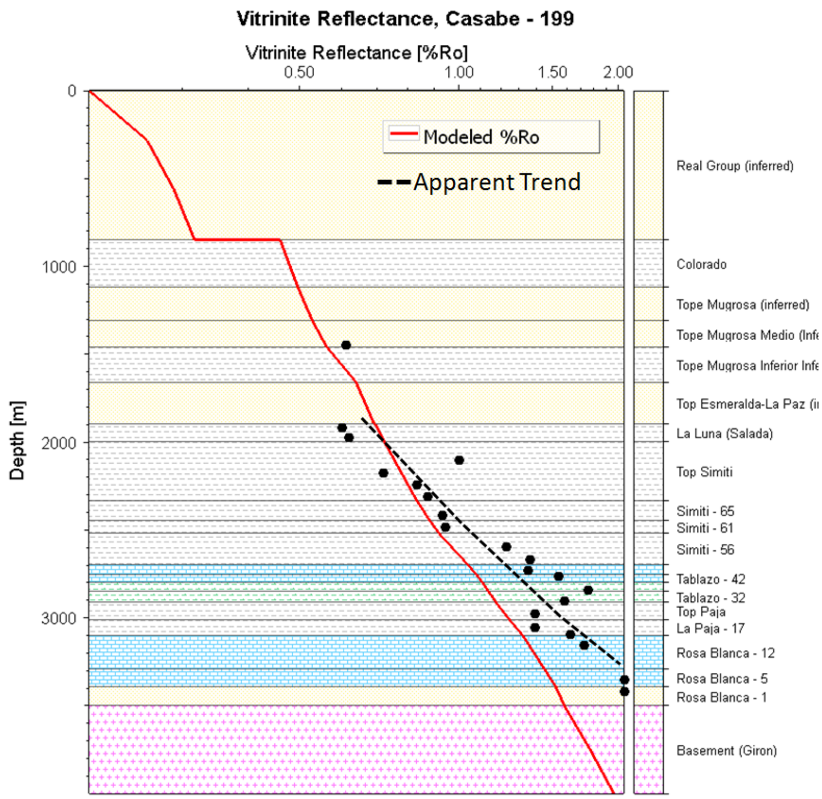

Figure 5. Predicted and observed vitrinite reflectance (%R_o) for the Casabe 199 well, which was modeled using similar of the basin history inputs as used for the Infantas 1613 well. Deviation of modeled %R_o from calibration data shows that uncertainty in model inputs still exists.

References

Cooper, M., et al. “Basin Development and Tectonic History of the Llanos Basin, Eastern Cordillera, and Middle Magdalena Valley, Colombia.” *AAPG Bulletin*, v. 79, no. 10, (1995): 1421-1443.

Eslinger, E., et al. “Probabilistic Facies Assignments in the La Luna Formation, Middle Magdalena Basin, Colombia, from Standard Well Logs Using Whole Core CT Scan Data as Initialization Input.” *AAPG Unconventional Resources Technology Conference* (2014).

Galvis-Portilla, H., et al. “Regional Sequence Stratigraphy of the Upper Cretaceous La Luna Formation in the Magdalena Valley Basin, Colombia.” *AAPG Unconventional Resources Technology Conference* (2014).

Gomez, E., Jordan, T., Allmendinger, R., Hegarty, K., Kelley, S., and Heizler, M. “Controls on architecture of the Late Cretaceous to Cenozoic southern Middle Magdalena Valley Basin, Colombia.” *GSA Bulletin*, v. 115, no. 2, (2003): 131-147.

Goncalves, F., Garcia, D., Penteado, H., Giraldo, B., Bedregal, R., and Gomez, P. “Cinetica De La Generacion Del Petroleo: Principios Y Aplicacion En Las Cuencas Colombianas.” *CT&F*, v. 2, no. 2, (2001): 27-41.

Horton, B., Parra, M., Saylor, J., Nie, J., Mora, A., Torres, V., Stockli, D., and Strecker, M. “Resolving uplift of the northern Andes using detrital zircon age signatures.” *GSA Today*, v. 20, no. 7, (2010): 4-9.

Marcano, F., and Leonard, J. “Total Play Fairway Analyses and Recommendations of Hydrocarbon Volume in Unconventional Cretaceous Plays in the Eastern Cordillera, Colombia: A New Frontier.” *AAPG Unconventional Resources Technology Conference* (2014).

Moretti, I., Charry, G., Morales, M., and Mondragon, J. “Integrated exploration workflow in the south Middle Magdalena Valley (Colombia).” *Journal of South American Sciences*, v. 29, (2010): 187-197.

Peters, K., Burnham, A., and Walters, C. “Petroleum generation kinetics: Single versus multiple heating-ramp open-system pyrolysis.” *AAPG Bulletin*, v. 99, no. 4, (2015): 591-616.

Ramon, J., and Dzou, L. “Petroleum geochemistry of Middle Magdalena Valley, Colombia.” *Organic Geochemistry*, v. 30, (1999): 249-266.

Ramon, J., Dzou, L., Hughes, W., and Holba, A. “Evolution of the Cretaceous organic facies in Colombia: implications for oil composition.” *Journal of South American Earth Sciences*, v. 14, (2001): 31-50.

Rangel, A., Parra, P., and Nino, C. “The La Luna formation: chemostratigraphy and organic facies in the Middle Magdalena Basin.” *Organic Geochemistry*, v. 31, (2000): 1267-1284.

Rangel, A., Moldowan, J., Nino, C., Parra, P., and Giraldo, B. "Umir Formation: Organic geochemical and stratigraphic assessment as cosource for Middle Magdalena basin oil, Colombia." *AAPG Bulletin*, v. 86, no. 12, (2002): 2069-2087.

Reyes-Harker, A., et al. "Cenozoic paleogeography of the Andean foreland and retroarc hinterland of Colombia." *AAPG Bulletin*, (2014). **Preliminary Version*

Veiga, R., and Dzelalija, F. "A Regional Overview of the La Luna Formation and the Villeta Group as Shale Gas/Shale Oil in the Catatumbo, Magdalena Valley and Eastern Cordillera Regions, Colombia." *Search and Discovery Article*, no. 10565, (2014).

Villamil, T. "Regional Hydrocarbon Systems of Colombia and Western Venezuela: Their Origin, Potential, and Exploration." *In* C. Bartolini et al., eds., The Circum-Gulf of Mexico and the Caribbean: Hydrocarbon habitats, basin formation, and plate tectonics: AAPG Memoir 79, p. 697-734 (2003).

Walls, J., Ceron, M., and Anderson, J. "Characterizing Unconventional Resource Potential in Colombia; a Digital Rock Physics Project." *AAPG Unconventional Resources Technology Conference* (2014).

Zumberge, J. "Source Rocks of the La Luna Formation (Upper Cretaceous) in the Middle Magdalena Valley, Colombia." (1984).

CHARACTERIZING THE EXHUMATION PATH OF THE FIRST ULTRAHIGH-PRESSURE TERRANE IN NORTH AMERICA

Zachary F. M. Burton[1] and Emily M. Peterman
Department of Earth and Oceanographic Science, Bowdoin College
[1]Now at: *Department of Geological Sciences, Stanford University*

Although the Appalachians formed one of the largest mountain belts on Earth, their early history remains elusive in large part because this early history has been overprinted. Garnet-kyanite-cordierite schist units cropping out on the western margin of the Goshen Dome of western Massachusetts provide a valuable window into these earliest phases of Appalachian mountain building. In this study, we used laser ablation split-stream inductively coupled plasma-mass spectrometry (LASS-ICP-MS) and electron probe micro-analyzer (EPMA) wavelength-dispersive x-ray spectrometry (WDS) data from monazite included in two garnet-kyanite-cordierite schists. These data yield a metamorphic history from ~395 to 355 Ma constructed via the integration of U-Pb ages, rare earth element (REE) distributions, Gd/Yb ratios, Yttrium compositional maps (Figure 1), and host phase population distributions.

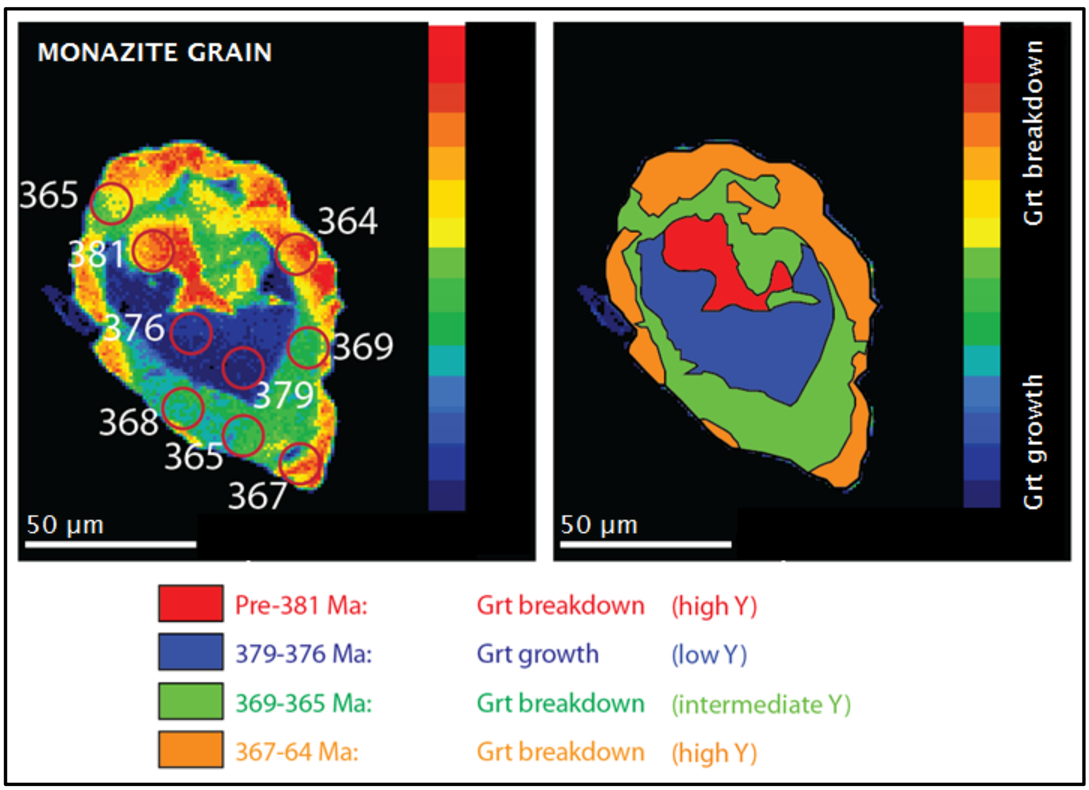

Figure 1. (a) EPMA WDS compositional map and (b) sketch of Yttrium (Y) concentrations for a representative monazite grain highlighting the presence of multiple, distinct chemical domains; red circles show location of and age from LASS-ICP-MS spot analyses; color is scaled for total range of Y intensity for the 219 monazite grains analyzed; below the map and sketch is a timeline illustrating how U-Pb dates and REE and trace element data are integrated to build a tectonic history.

This metamorphic history is characterized by a period of relic ultrahigh-pressure (UHP) garnet breakdown from ~396 to 383 Ma, a period of garnet growth from ~383 to 369 Ma concomitant with fluid pulsing/anatexis likely related to the high-T Acadian thermal event, and a second period of garnet breakdown from ~369 to 355 Ma (Figure 2). The schists share similar histories of exhumation, however the timing of early (pre-383 Ma) retrograde reactions is offset between the two samples by ~5 Myr. This suggests that the schist units came together at ~383 Ma during exhumation from UHP conditions to the mid-crust.

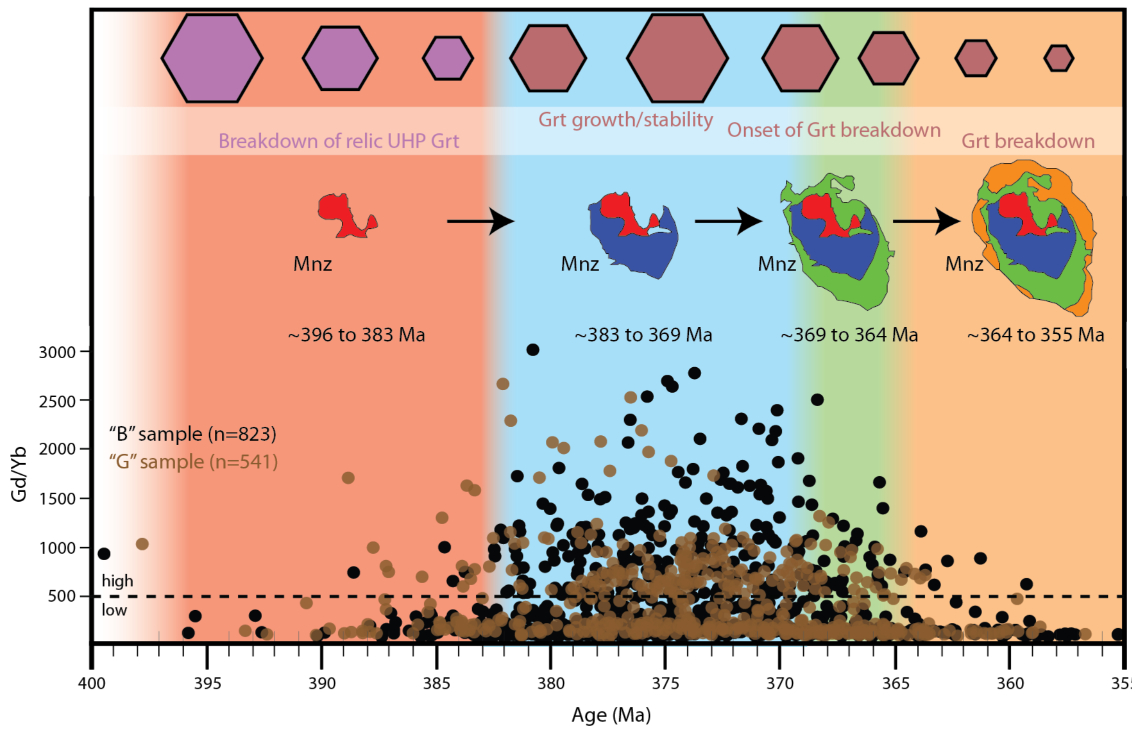

Figure 2. Timeline of garnet ("Grt" above) evolution as revealed by monazite ("Mnz" above) compositional domains, Gd/Yb ratios (black and brown scatterplot points), and HREE slopes; garnet evolution shown by purple (UHP garnet) and maroon (post-UHP garnet) hexagons at top of frame.

This study presents the first nearly continuous record of metamorphism during the early phases of mountain building in the Appalachians and provides valuable insight into exhumation processes of UHP terranes.

STOCHASTIC MULTISCALE ELECTROFACIES CLASSIFICATION OF WELL LOGS AS A PRELUDE TO HIGH-RESOLUTION BASIN AND PETROLEUM SYSTEM MODELING

Mustafa Al Ibrahim[1], Tapan Mukerji[1], and Allegra Hosford Scheirer[2]
[1]*Department of Energy Resources Engineering, Stanford University*
[2]*Department of Geological Sciences, Stanford University*

Lithofacies classification is commonly used as a stepping stone to property propagation and upscaling. The classification workflows used in industry are mostly deterministic and they do not incorporate uncertainty analysis. Thus, geomodeling workflows are forced to incorporate well data as hard data. This study presents a stochastic multi-scale workflow for electrofacies classification. The ultimate objective is to extend this stochastic well log classification to seismic. The three-dimensional model will then be statistically populated with different properties, such as total organic carbon content, and used in basin and petroleum system modeling applications.

The workflow presented here extends existing workflows by using a combination of statistical methods including unsupervised neural network self-organizing maps, principal component analysis, k-means clustering, and hierarchal clustering. In this workflow, data are normalized and principal component analysis is applied to extract independent variables to remove any unintentional bias in the data (e.g. the fact that both the density and neutron logs are proportional to porosity). Next, self-organizing maps or k-means clustering are used to create the initial classification space. Hierarchal clustering is used to study the relationship between the nodes in the classification space and build the upscaling tree. Measurements from the same training dataset or from another dataset assuming stationarity are then classified stochastically based on a distance measurement between the model classification space and the data. Different realizations are created and a probabilistic score is calculated for them. In addition, the most likely realization is also calculated and compared to other realizations. The multi-scale visualization of realizations allows for the identification of important lithological changes and small scale vertical heterogeneity at the same time. Planned extensions include the inclusion of vertical spatial component to the classification through the use of hidden Markov chains and optimizing parameters automatically. Integration of results with seismic data might be complicated due to scale differences.

The developed workflow is applied on a shale interval from North Slope, Alaska. Five key electrofacies are identified. Results are validated using conventional geologic description of the core at the same well (Figure 1). There is a general agreement between core-derived lithofacies and well-log derived electrofacies. The different realizations of the electrofacies classifications show small-scale heterogeneities (i.e. uncertainties) that are generally not incorporated in basin and petroleum system modeling (Figure 2). Whether or not these heterogeneities are important is currently being investigated. If they are, there is a need to perform high-resolution basin and petroleum system modeling. If that is not technically feasible because of computational power, then the best effective value for each property in the model needs to be defined using statistical methods. If there is a lack of data, statistical models based on physical process should define the distribution of each property.

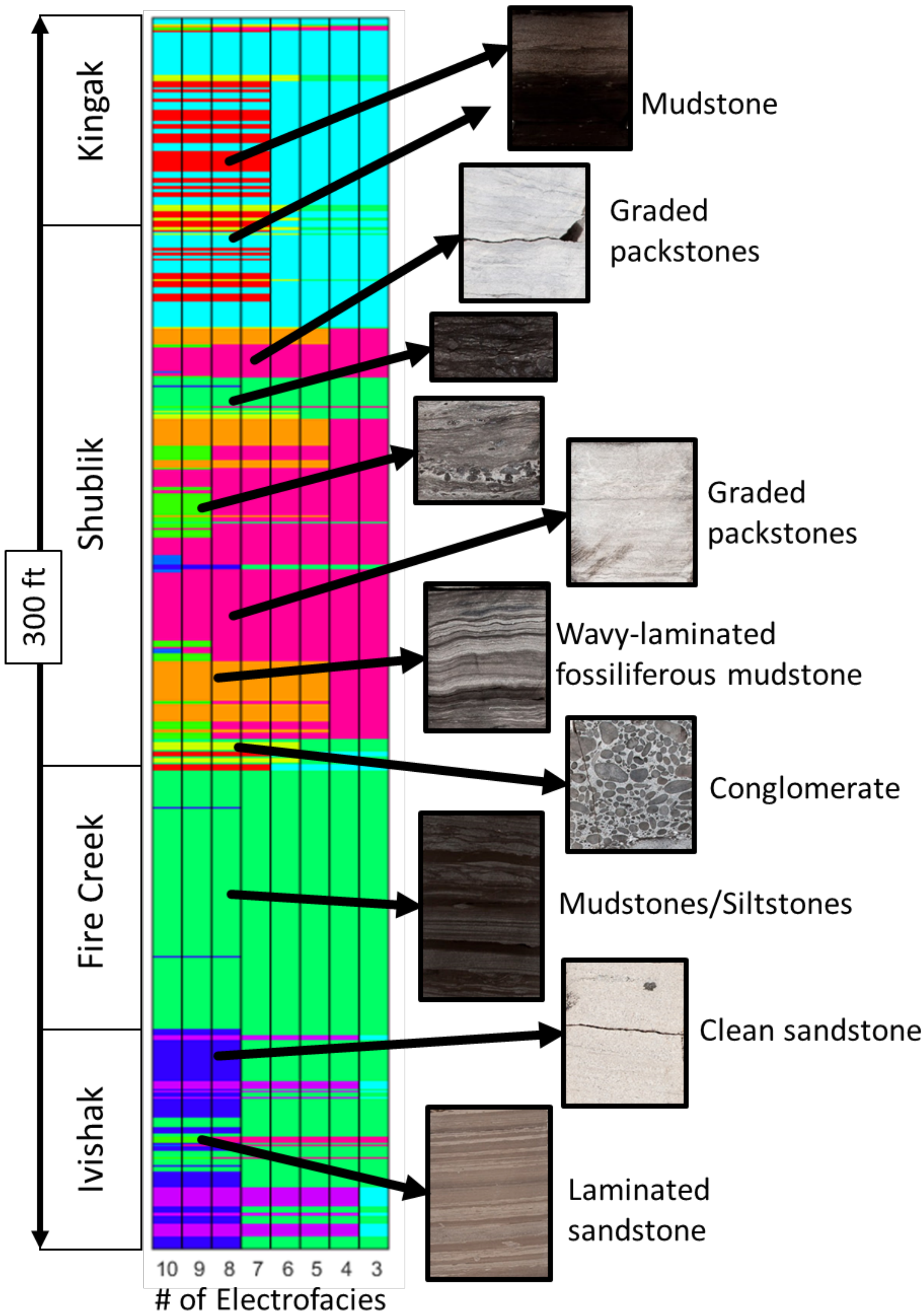

Figure 1. Core lithofacies variations correlated with results from electrofacies analysis.

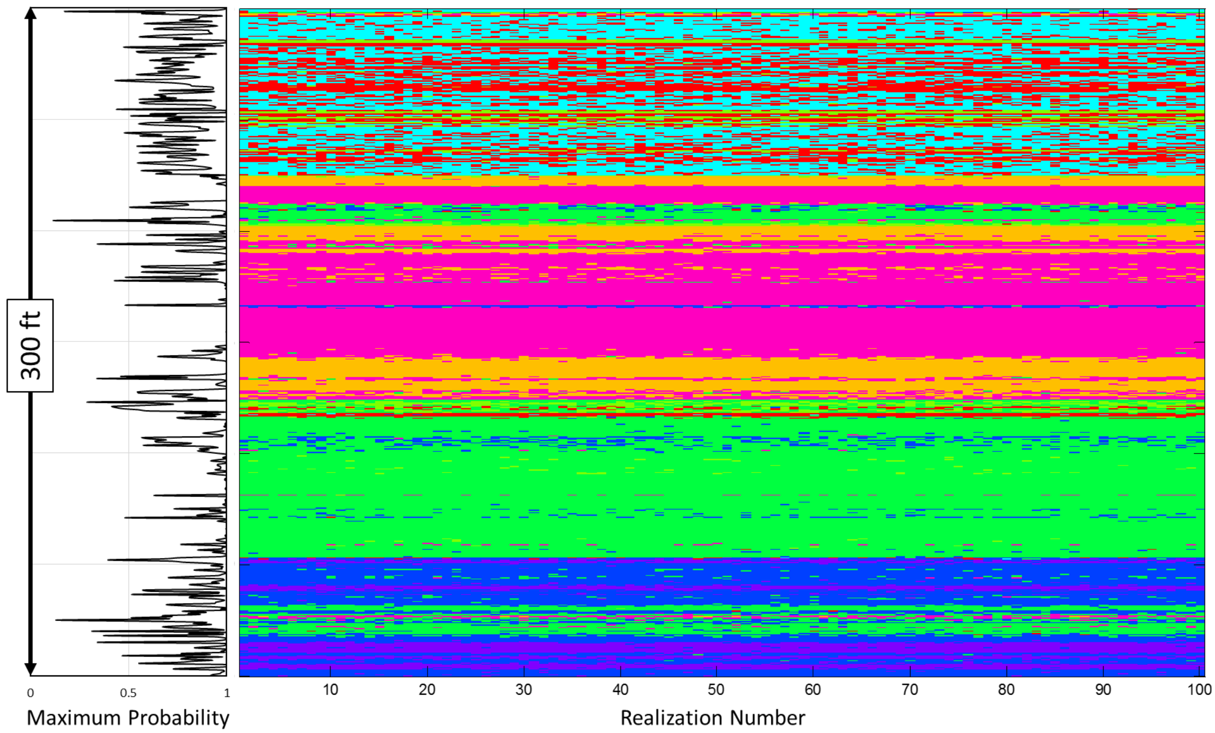

Figure 2. Example of 100 stochastic realizations defined for one well. Different colors define different electrofacies. There is more realization-to-realization variability when the probability for the most likely category is close to the probabilities for the other categories.

3D BASIN AND PETROLEUM MODELING OF THE PICEANCE BASIN AND SOURCE ROCK MATURATION HISTORY

Yao Tong[1], Carolyn Lampe[2], Steve Graham[3], Allegra Hosford Scheirer[3], Les Magoon[3], and Tapan Mukerji[1]
[1]*Department of Energy Resources Engineering, Stanford University*
[2]*ucon geoconsulting*
[3]*Department of Geological Sciences, Stanford University*

Abstract

In this study, we construct a three dimensional basin model for the Piceance Basin in order to study the evolution and corresponding source rock maturation history of the basin. From Late Cretaceous to Present day, the study area went through multiple geodynamic processes, the most significant of which was a transition from a marine depositional basin into a terrestrial basin subject to uplift and erosion. Multiple data sets were integrated to reconstruct sediment burial, compaction, uplift, and erosion. Source rock maturation history, impacted by the complicated basin geological history, was also investigated.

Geologic Background of the Piceance Basin

The Piceance Basin is an intermontane basin located in northwest Colorado. During the Cretaceous, the region was part of the expansive epicontinental Western Interior Seaway, which subsequently was uplifted and partitioned as a discrete sedimentary basin during the late Cretaceous through Eocene Laramide orogeny (Johnson and Nuccio, 1986, 1993). Several Laramide uplifts and arch structures define the basin (Figure 1). Today, the basin is bounded by the White River uplift to the east, Douglas Creek arch to the west, Uncompahgre uplift to the southwest, Axial Basin anticline to the northeast, Gunnison Uplift to the southeast, and Uinta Mountains to the northwest. The basin is highly asymmetric with steeply dipping strata on the eastern flank and gently dipping strata on the western and southwestern part of the basin (Figure 1). The steeply dipping eastern flank, the Grand Hogback, was formed by deeper west-vergent reverse or thrust faults (Johnson and Nuccio, 1986; Nuccio and Johnson, 1989; Johnson and Roberts, 2003). On the west flank, the Douglas Creek Arch separates the Piceance Basin from the Uinta Basin.

The stratigraphic sequence has a major transition from shallow marine, coastal plain sediments deposited during the Upper Cretaceous to terrestrial sediments (highly uplifted and eroded) deposited during the Tertiary (Figure 2). Within the Upper Cretaceous strata, the thick (> 1500 m) marine shale of the Mancos Group was deposited above the Lower Cretaceous Dakota Formation. These sediments are then overlain by the Mesaverde Group, which is the primary reservoir of the basin's tight-gas resources and is composed, in ascending order, of Castlegate, Sega, Iles and Williams Fork Formations (Johnson, 1989). The widespread Cameo Coal occurs at the top of the Iles Formation, and is believed to be the major source rock for the extensive gas resources within the overlying Williams Fork Formation tight sandstone (Soeder et al., 1987; Fall et al., 2012, 2014). Overlying

Tertiary strata include Wasatch (Paleocene-Eocene), Green River (lower Eocene) and Uinta (upper Eocene) formations.

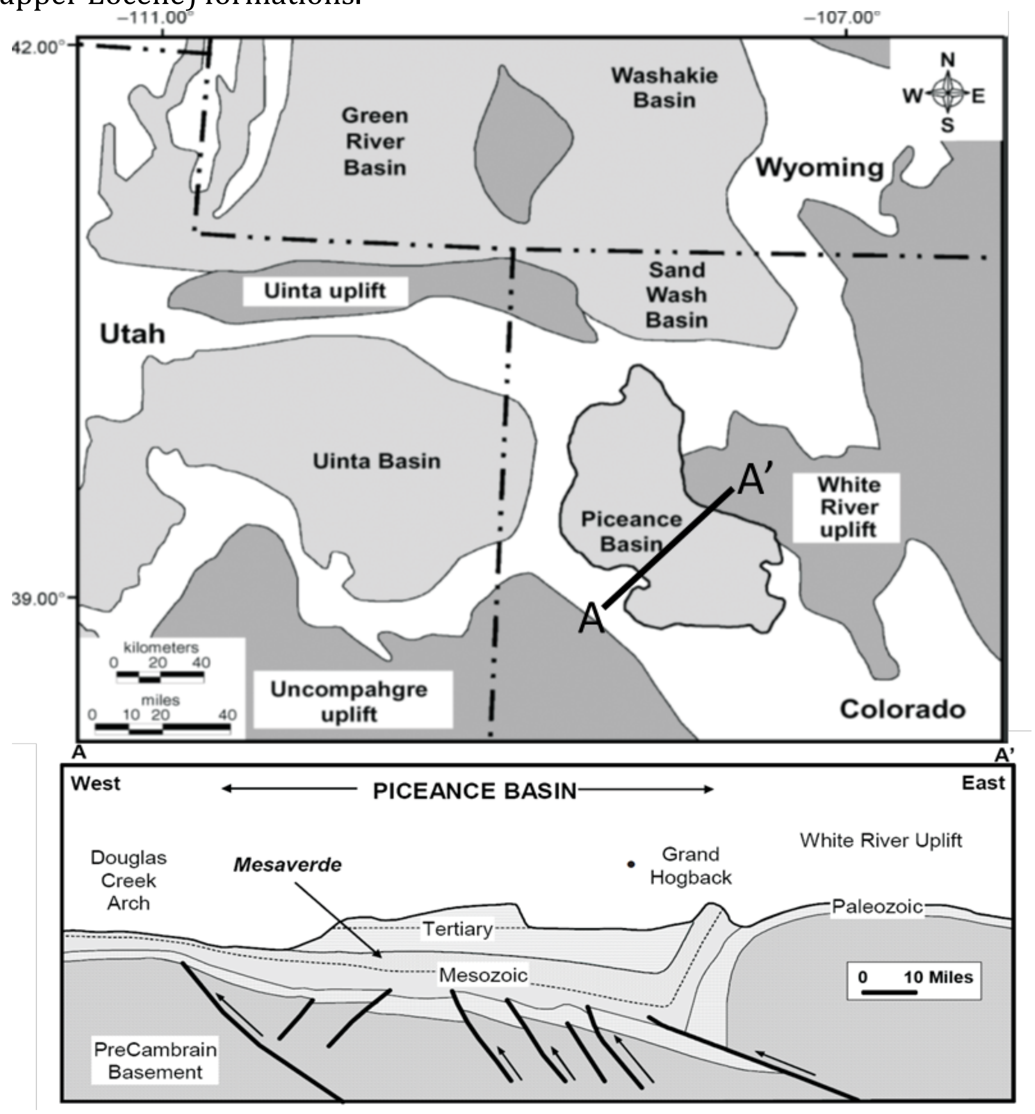

Figure 1. Piceance Basin location and major structures define the basin boundary. The lower chart shows the cross section of the Piceance Basin and adjacent basement uplifts in western Colorado. Modified from (Wilson et al., 2003).

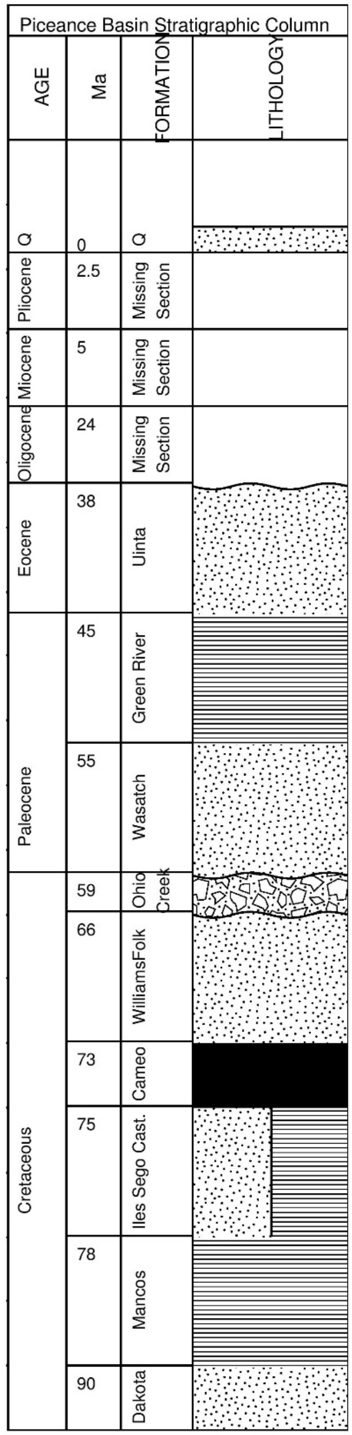

Figure 2. Piceance Basin stratigraphic column

Basin Modeling
Present Day Basin Geometry

The basin model includes sediment layers from Late Cretaceous to Present-day, including Dakota group, Mancos Shale, Rollins Sandstone, Cameo Coal, Mesaverde-Williams Fork Formation, Wasatch Formation, Green River Formation, and Uinta Formation. Present day geometry was first constructed using previous regional studies and available well data. A regional structure contour of the Rollins Sandstone Member (and its equivalent, the Trout Creek Sandstone Member) was used as a reference map for reconstructing the basin-wide present geometry (Figure 3).

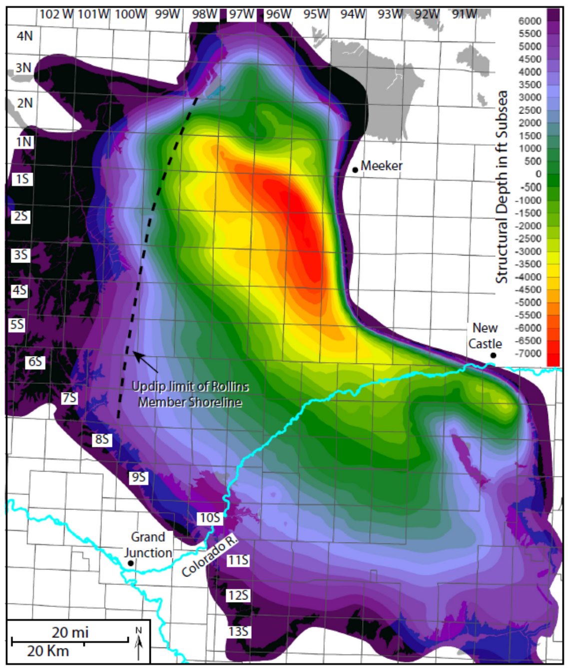

Figure 3. Structure map of the top of the Rollins Member of the Iles Formation, Piceance Basin. Contour interval is 500 foot (152 meter). Black shows the outcrop distribution of the Williams Fork Formation (Leibovitz, 2010).

Basin Burial History and Uplift/Erosion Modeling

Our study area has gone through complicated structural and tectonic events. Multiple phases of uplift and erosion occurred throughout the basin history and impact the basin subsidence and burial history. Considering our work scope and study interests, two major uplift/erosion events are included (Figure 4) in the model. The first uplift event was modeled from 67 to 63 Ma to represent the onset of the Laramide Orogeny and its resulting uplifted structures (White River Uplift on the east and Douglas Creek Arch on the west). An erosional event was also created to model the regional Cretaceous-Tertiary unconformity in the study area. The second uplift and erosion event was modeled from 10 Ma to Present day; this features downcutting by the Colorado River (Johnson and Nuccio, 1986; Mix et al., 2011; Snell et al., 2014).

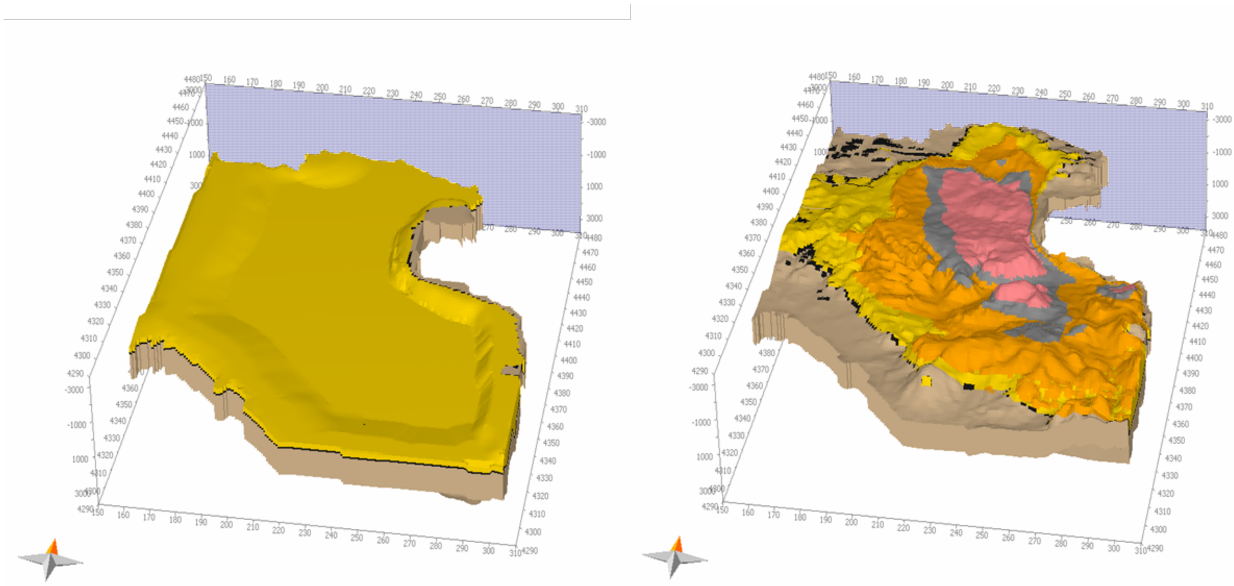

Figure 4. Two uplift and erosion events in the Piceance Basin model. Left: onset of Laramide Orogeny and erosion created K-T unconformity; Right: recent regional uplift and erosion from Colorado River.

Source Rock Maturation History

Thermal maturation history of the source rock is closely related to the burial, compaction, and uplift/erosion history of the sedimentary basin. In this model we focus on the maturation history of the regional Cameo Coal (Figure 5), a source rock that contains mainly type III kerogen (Johnson and Rice, 1990; Yurewicz et al., 2003; Zhang et al., 2008). The Cameo Coal was deposited during the Late Cretaceous (~72 Ma) and subsequently buried during a period of basinal subsidence. The first uplift and erosion event does not impact the source rock maturation significantly. As the Williams Fork formation and other Late Cretaceous strata overlie the source rock, the weathering at the Cretaceous-Tertiary unconformity initially took away sediments from the overburden formations. Later, as the Piceance Basin was filled with fluvial and lacustrine deposits of the Paleocene Wasatch and Eocene Green River Formations, the source rock gradually reached the maturation window. Miocene strata are generally missing in the study area due to erosion, however, the missing section adds to the total overburden on the Cameo Coal source rock during this period of time.

The onset of gas generation in our basin model occurred during the early Paleocene and continued to Miocene times. From the Miocene to Pliocene, major tectonism resumed and the entire region was uplifted vertically (Johnson and Nuccio, 1986; Nuccio and Johnson, 1989). Downcutting of strata by the Colorado River beginning about 9 Ma removed as much as 5000 feet of overburden from the central part of the basin (Johnson and Nuccio, 1986), resulting in the cessation of hydrocarbon generation.

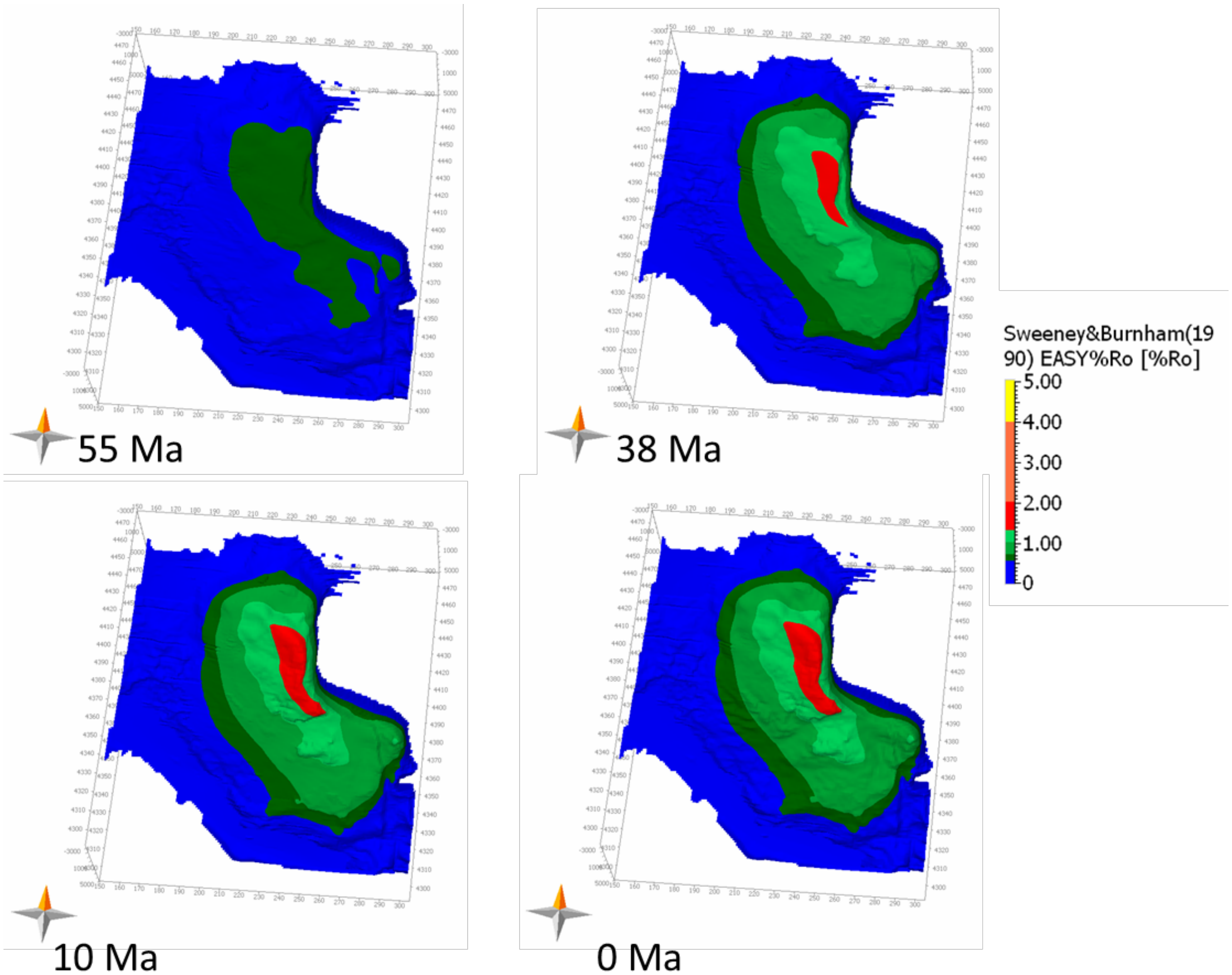

Figure 5. Source rock maturation maps from Paleocene to present day.

References

Cole, R., and S. Cumella, 2003, Stratigraphic architecture and reservoir characteristics of the Mesaverde Group, southern Piceance Basin, Colorado.

Fall, A., P. Eichhubl, R. J. Bodnar, S. E. Laubach, and J. S. Davis, 2014, Natural hydraulic fracturing of tight-gas sandstone reservoirs, Piceance Basin, Colorado: *Geological Society of America Bulletin*, no. X, p. B31021.1–, doi:10.1130/B31021.1.

Fall, A., P. Eichhubl, S. P. Cumella, R. J. Bodnar, S. E. Laubach, and S. P. Becker, 2012, Testing the basin-centered gas accumulation model using fluid inclusion observations: Southern Piceance Basin, Colorado: *AAPG Bulletin*, v. 96, no. 12, p. 2297–2318, doi:10.1306/05171211149.

Johnson, R. C., 1989, Geologic History and Hydrocarbon Potential of Late Cretaceous-Age, Low-Permeability Reservoirs, Piceance Basin, Western Colorado: *USGS Bulletin* 1787-*E*.

Johnson, R. C., and V. F. Nuccio, 1993, MAP Showing General Geology selected vitrinite reflectance values, and locations of surface samples and drill holes used to construct vitrinite reflectance profiles, Uinta and Piceance basins and adjacent areas, Western Utah and Western Colorado.

Johnson, R. C., and V. F. Nuccio, 1986, Structural and Thermal History of the Piceance Creek Basin , Western Colorado, in Relation to Hydrocarbon Occurrence in the Mesaverde Group: Geology of tight gas reservoirs: *AAPG Studies in Geology* 24, p. 165–205.

Johnson, R. C., and D. D. Rice, 1990, Occurrence and geochemistry of natural gases, Piceance basin, Northwest Colorado: *American Association of Petroleum Geologists Bulletin*, v. 74, no. 6, p. 805–829, doi:10.1306/0C9B2399-1710-11D7-8645000102C1865D.

Johnson, R. C., and S. B. Roberts, 2003, The Mesaverde Total Petroleum System , Uinta-Piceance Province, Utah and Colorado: Chapter 7

Leibovitz, M. B., 2010, Sequence Stratigraphy of the Upper Cretaceous Upper Williams Fork Formation, Piceance Basin, Northwest Colorado, and its Contribution to the Basin-Centered Gas Accumulation: 169 p.

Mix, H. T., A. Mulch, M. L. Kent-Corson, and C. P. Chamberlain, 2011, Cenozoic migration of topography in the North American Cordillera: *Geology*, v. 39, p. 87–90, doi:10.1130/G31450.1.

Nuccio, V. F., and R. C. Johnson, 1989, Variations in Vitrinite Reflectance Values for the Upper Cretaceous Mesaverde Formation, Southeastern Piceance Basin, Northwestern Colorado-Implications for Burial History and Potential Hydrocarbon Generation: *USGS Bulletin*, p. 10.

Snell, K. E., P. L. Koch, P. Druschke, B. Z. Foreman, and J. M. Eiler, 2014, High elevation of the "Nevadaplano" during the Late Cretaceous: *Earth and Planetary Science Letters*, v. 386, p. 52–63, doi:10.1016/j.epsl.2013.10.046.

Soeder, D. J., P. L. Randolph, and others, 1987, Porosity, permeability, and pore structure of the tight Mesaverde Sandstone, Piceance Basin, Colorado: *SPE Formation Evaluation*, v. 2, no. 02, p. 129–136.

Wilson, M. S., K. W. Grove, and A. B. Wilson, 2003, Exploration of the Mississippian Leadville Limestone in the Piceance Basin, Western Colorado.

Yurewicz, D. A., K. M. Bohacs, J. D. Yeakel, and K. Kronmueller, 2003, Source Rock Analysis and Hydrocarbon Generation , Mesaverde Group and Mancos Shale, Northern Piceance Basin, Colorado, in *Piceance Basin Guidebook*: p. 130–153.

Yurewicz, D. A., J. Kendall, K. Kronmueller, T. C. Ryan, K. M. Bohacs, R. E. Klimentidis, M. E. Meurer, and J. D. Yeakel, 2008, Controls on Gas and Water Distribution, Mesaverde Basin-centered Gas Play, Piceance Basin, Colorado, in S. P. Cumella, K. W. Shanley, and W. K. Camp, eds., Understanding, exploring, and developing tight-gas sands—2005 Vail Hedberg Conference: *AAPG Hedberg Series*: p. 105–136, doi:10.1306/13131053H31639.

Zhang, E., R. J. Hill, B. J. Katz, and Y. Tang, 2008, Modeling of gas generation from the Cameo coal zone in the Piceance Basin, Colorado: *AAPG Bulletin*, v. 92, no. 8, p. 1077–1106, doi:10.1306/04020806015.

PREDICTING OVERPRESSURE USING BASIN MODELING SOFTWARE

Jens-Erik Lund Snee
Department of Geophysics, Stanford University

It is notoriously difficult to predict porosity and pore pressure in buried sedimentary rocks, particularly if these rocks have experienced a complex geologic history. Many techniques exist to estimate overpressure using geophysical imaging methods, but basin and petroleum system modeling (BPSM) software also holds great potential for making independent estimates of pore pressure, effective stress, and porosity due to its ability to model 3D geologic history.

I conducted two sets of simple tests to evaluate the capabilities of industry standard PetroMod software for predicting porosity and pore pressure. First, I attempted to replicate results of an isotropic rock compression experiment (Zimmer, 2004; Zimmer et al., 2007) using a basic 1D model (Figure 1). This 1D test highlights PetroMod's impressive ability to incorporate customized compaction criteria, but it also shows that the absence of elastic rebound significant limitations for realistically modeling porosity and pore pressure.

In the second set of experiments, I employed a simple 3D "layer cake" model in order to determine whether BPSM might reveal hard overpressure in sediments having otherwise normal porosity values that might hence go undetected using traditional geophysical overpressure detection methods. These tests found that the software is indeed able to model large fluctuations in pore pressure even as porosity remains constant over time. Thus, BPSM should be considered a valuable independent complement to other techniques for estimating pore pressure and porosity in the subsurface.

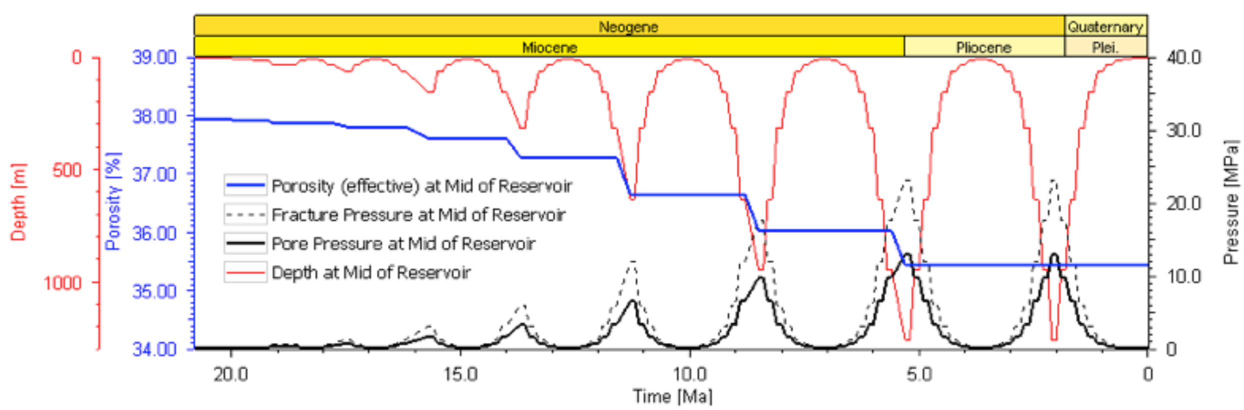

Figure 1: Results from a synthetic 1D reservoir loading and unloading experiment using BPSM software, which shows that modeled porosity does not rebound elastically during unloading steps, despite observations of this phenomenon in laboratory rock physics experiments (e.g., Zimmer et al., 2007; Zoback, 2010).

Although these simple experiments do not account for natural pore pressure- and stress-induced fault-valve behaviors known to occur in the subsurface (e.g., Townend and Zoback, 2000; Finkbeiner et al., 2001; Zoback and Townend, 2001; Sutherland et al., 2012; Lund Snee et al., 2014; Burgreen-Chan et al., 2015), the 3D tests also reveal apparent artifacts in PetroMod's modeling of porosity evolution. For example, during burial and development of hard overpressure, a porous reservoir unit is neither compacted nor decompacted, instead showing an unrealistically stable porosity evolution (Figure 2). This result thus illustrates a significant limitation in existing software for modeling compaction and fluid pressure evolution. The effectiveness of BPSM for modeling porosity and pore pressure will increase as future software releases resolve some apparent artifacts in compaction modeling and incorporate the capability to model additional geologic processes.

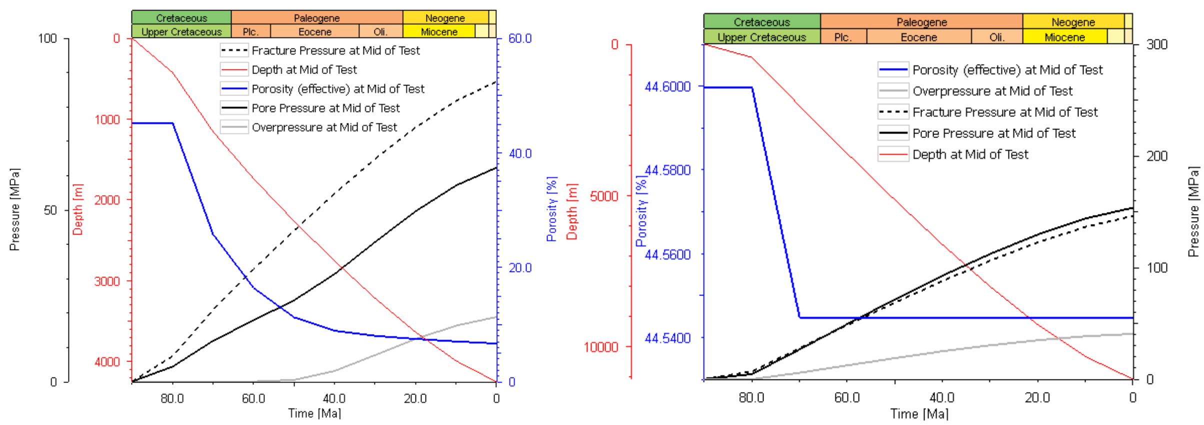

Figure 2. Results from one of the synthetic 3D reservoir burial experiments ("Experiment 2"), showing the effect of (A) permeable and (B) impermeable overburden and underburden on pore pressure and porosity evolution. In model (A), the reservoir unit is surrounded by overburden and underburden having moderate permeability values, which limits overpressure development and allows porosity to decrease asymptotically during burial and compaction. In contrast, model (B) incorporates completely impermeable overburden and underburden, which prevents dissipation of pore pressure, allowing overpressure to develop and preventing compaction. The porosity evolution shown in (B) is unrealistically stable and may illustrate an important artifact in PetroMod software, in which neither compaction nor decompaction occurs in the presence of hard overpressure.

References

Burgreen-Chan, B., Meisling, K.E., Graham, S.A., 2015. Basin and petroleum system modelling of the East Coast Basin, New Zealand: a test of overpressure scenarios in a convergent margin. *Basin Res.* 1–32. doi:10.1111/bre.12121

Finkbeiner, T., Zoback, M.D., Flemings, P., Stump, B., 2001. Stress, pore pressure, and dynamically constrained hydrocarbon columns in the South Eugene Island 330 field, northern Gulf of Mexico. *Am. Assoc. Pet. Geol. Bull.* 85, 1007–1031.

Lund Snee, J.-E., Toy, V.G., Gessner, K., 2014. Significance of brittle deformation in the footwall of the Alpine Fault, New Zealand: Smithy Creek Fault zone*. J. Struct. Geol*. 64, 79–98. doi:10.1016/j.jsg.2013.06.002

Sutherland, R., Toy, V.G., Townend, J., Cox, S.C., Eccles, J.D., Faulkner, D.R., Prior, D.J., Norris, R.J., Mariani, E., Boulton, C., Carpenter, B.M., Menzies, C.D., Little, T. a., Hasting, M., De Pascale, G.P., Langridge, R.M., Scott, H.R., Reid Lindroos, Z., Fleming, B., Kopf, J., 2012. Drilling reveals fluid control on architecture and rupture of the Alpine fault, New Zealand. *Geology* 40, 1143–1146. doi:10.1130/G33614.1

Townend, J., Zoback, M.D., 2000. How faulting keeps the crust strong. *Geology* 28, 399–402. doi:10.1130/0091-7613(2000)28<399:HFKTCS>2.0.CO

Zimmer, M.A., 2004. Seismic velocities in unconsolidated sands: Measurements of pressure, sorting, and compaction effects [WWW Document]. URL http://adsabs.harvard.edu/abs/2004PhDT.......417Z

Zimmer, M.A., Prasad, M., Mavko, G., Nur, A., 2007. Seismic velocities of unconsolidated sands: Part 2 — Influence of sorting- and compaction-induced porosity variation. *Geophysics* 72, E15. doi:10.1190/1.2364849

Zoback, M.D., 2010. *Reservoir geomechanics*. Cambridge University Press.

Zoback, M.D., Townend, J., 2001. Implications of hydrostatic pore pressures and high crustal strength for the deformation of intraplate lithosphere. *Tectonophysics* 336, 19–30. doi:10.1016/S0040-1951(01)00091-9

THE IMPACT OF ALLOCHTHONOUS SALT EVOLUTION AND OVERPRESSURE DEVELOPMENT ON THE PETROLEUM SYSTEM IN THE THUNDER HORSE MINI-BASIN

Wisam AlKawai[1], Tapan Mukerji[2], and Stephan Graham[1]
[1]*Department of Geological Sciences, Stanford University*
[2]*Department of Energy Resources Engineering, Stanford University*

This study focuses on the south-central Mississippi Canyon (MC) (Figure 1), a feature that is centered on the Thunder Horse intraslope mini-basin (Figure 2). This mini-basin formed by localized salt withdrawal and later inverted into a turtle structure with further salt withdrawal along the flanks (Lapinski et al., 2004). Understanding the impact of allochthonous salt evolution and overpressure on source rock thermal maturity and migration pathways together with the impact of allochthonous movement on reservoir architecture is critical for future exploration in the Gulf of Mexico basin and similar salt-dominated basins (McBride et al., 1998; Rowan and Weimer, 1998; Stover et al., 2001; Hood et al., 2002). Some objectives of the study are to: (1) evaluate the impact of allochthonous salt movement on reservoir architecture, (2) contrast pore pressure development by multiple potential mechanisms, and (3) understand the impact of allochthonous salt evolution and overpressure on the source rock maturation and hydrocarbon migration pathways.

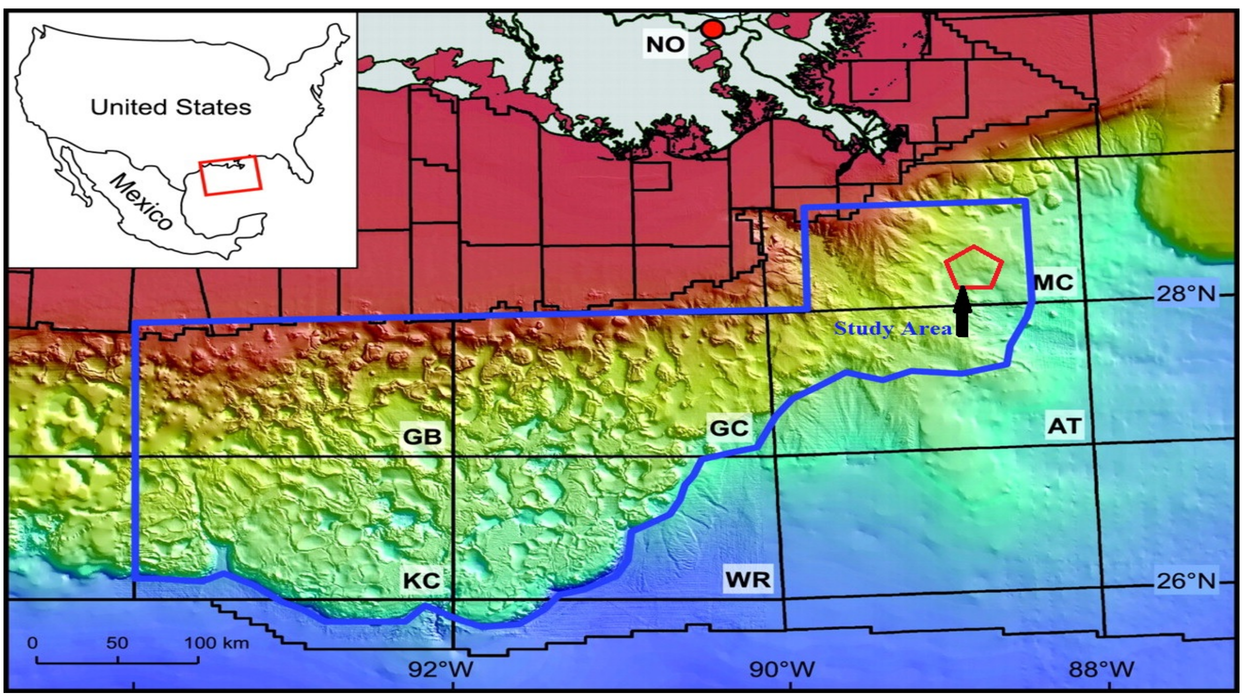

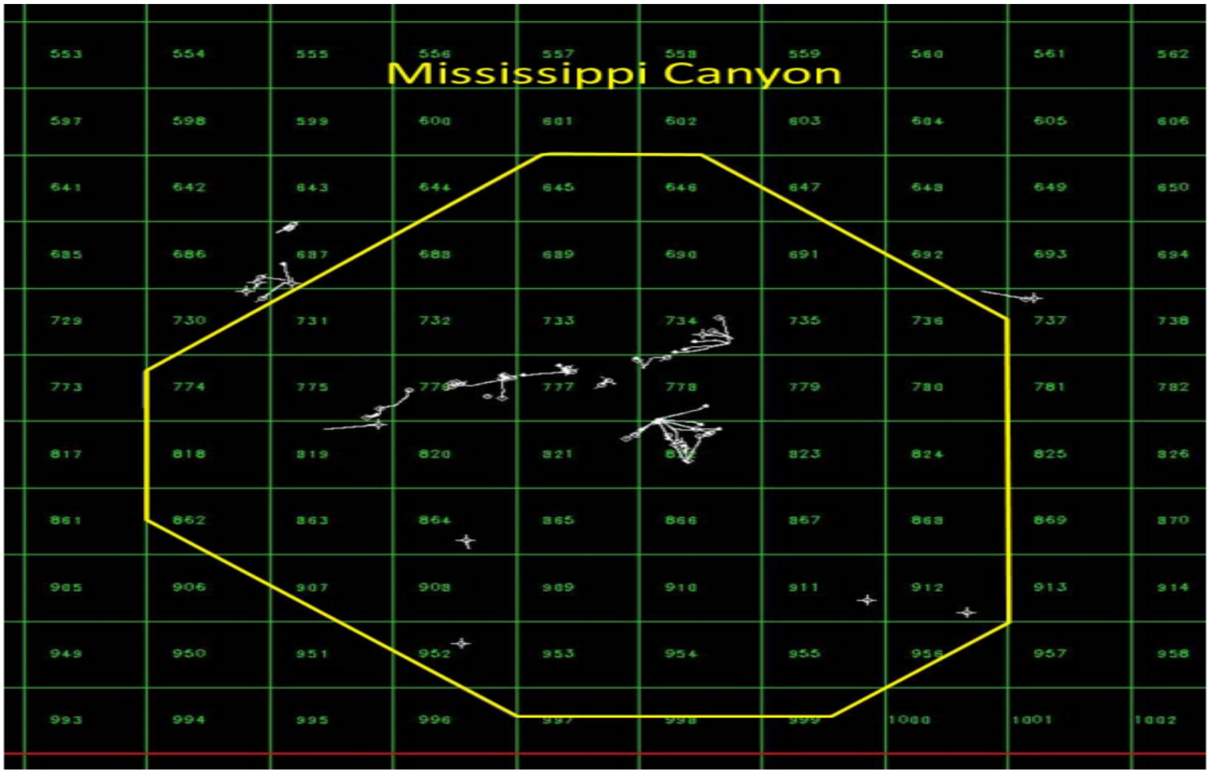

Figure 1. Location of the study area shown on a bathymetry map (a) and illustration of the blocks included in the seismic volume (b).

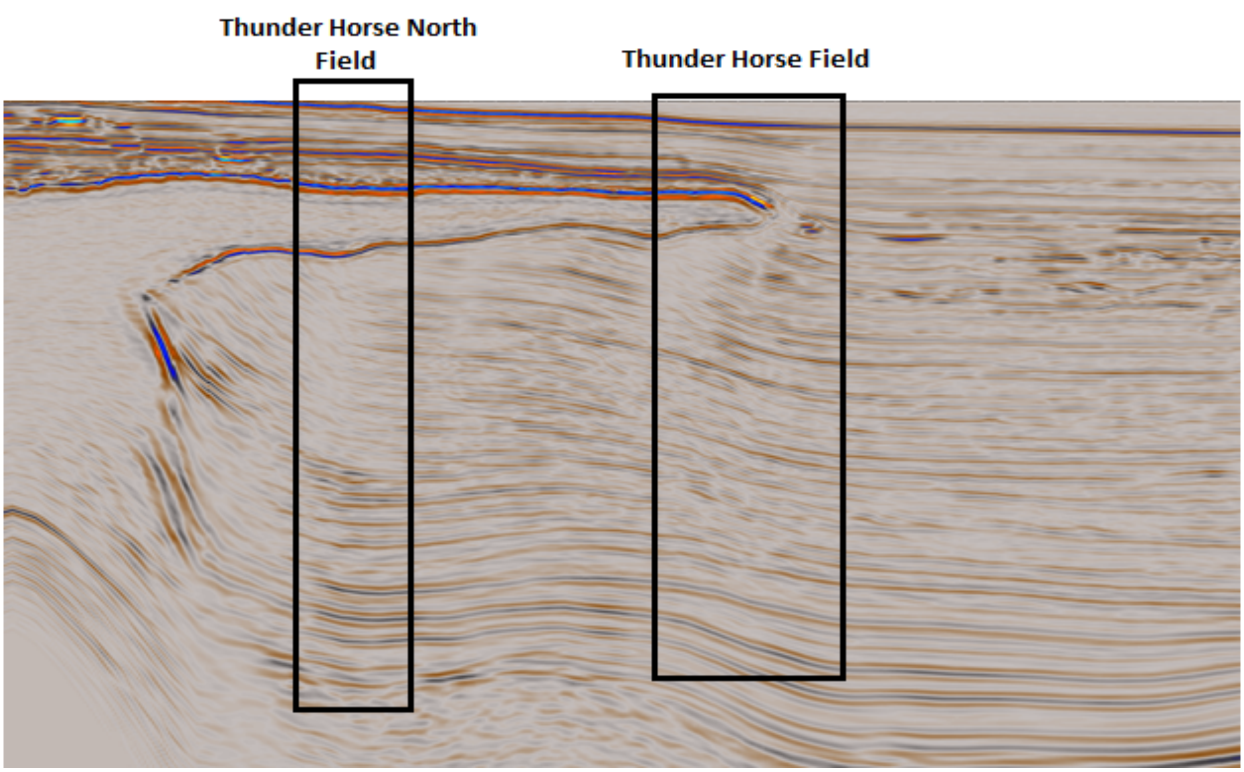

Figure 2. Seismic line showing the turtle structure of the Thunder Horse intraslope mini-basin.

Although some studies, such as Diaz et al. (2010) and Lapinski et al. (2004), documented the stratigraphic evolution in the Thunder Horse mini-basin from 99 Ma to present, there is still no detailed documentation of the reservoir architecture, the lithofacies distribution, or isopach thickness. These factors may impact hydrocarbon recovery in the Thunder Horse and Thunder Horse North fields. Also, further study may provide additional detailed insights into the effects of salt movement on reservoir architecture in the mini-basin province, which is important for future exploration in the northern Gulf of Mexico Basin. The first part of the study aims to provide a detailed description of the architecture of the main reservoirs through quantitative seismic interpretation (QSI). We will combine this description with interpreted thickness changes through time of both allochthonous and autochthonous salt to understand the effects of salt evolution on the reservoir architecture.

Looking at the turtle structure in Figure 2, there are differences in the burial history of the reservoirs between the Thunder Horse and Thunder Horse North fields. At the start of QSI, we defined probability density functions (PDFs) of the elastic properties of the reservoir lithofacies based on wells from both fields such those shown in Figure 3. The PDFs show differences in the separation of sandstone and shale between the two fields. This separation can be related to the compaction effect shown in Figure 4. Understanding this compaction trend is an important step to establish representative PDFs of the lithofacies. In addition, obtaining good quality inversion of the impedances of the reservoirs to classify the lithofacies and define the architecture of the main reservoirs is also important. We inverted the post-stack seismic data to obtain acoustic impedance cubes in the reservoir intervals and used wells from both fields for careful inversion and quality control. An example of the resulting impedance is shown in Figure 5, which shows good quality in terms of correlation with seismic data and with the acoustic impedances derived from wells. Future work will continue the QSI process and salt movement analysis to map and understand reservoir architecture development.

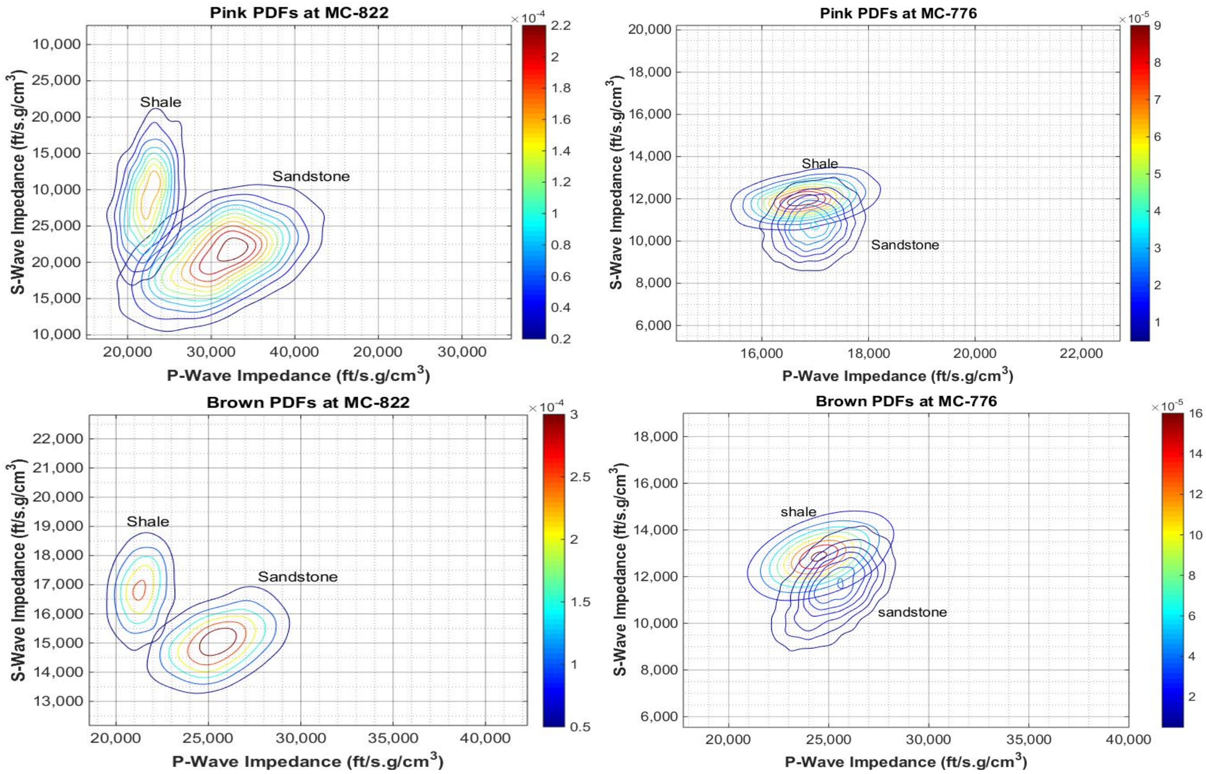

Figure 3. Bivariate PDFs of the impedances of two reservoir intervals in the Thunder Horse (right) and Thunder Horse North (left) Fields.

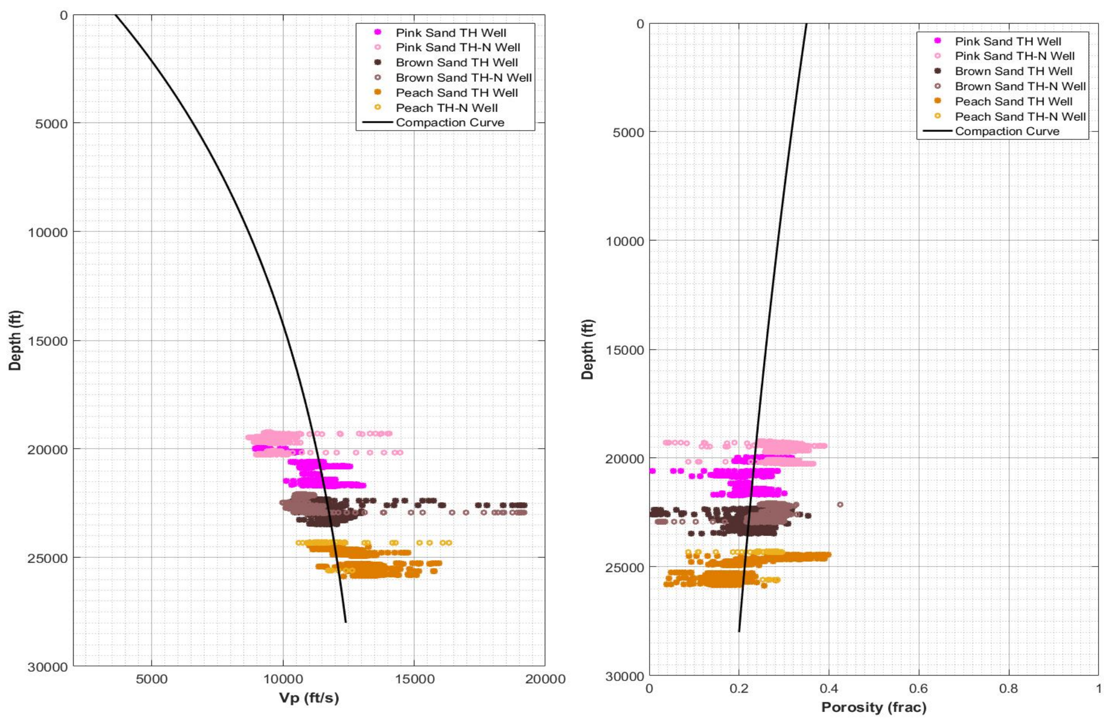

Figure 4. Compaction trends of the velocity and porosity of the reservoir sandstones; Cross Correlation with the original seismic=0.9745.

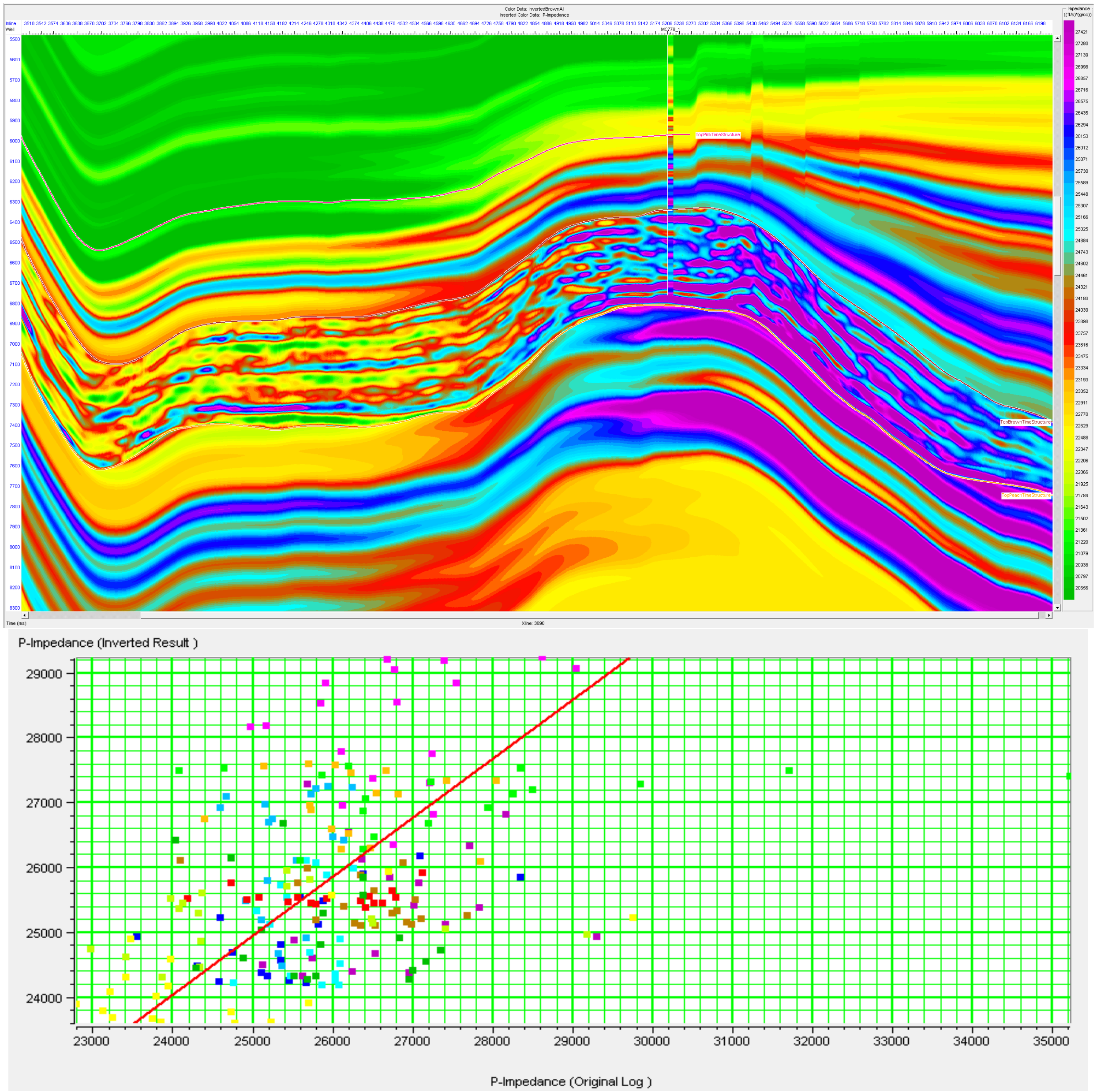

Figure 5. Inverted acoustic impedance for one of the reservoir zones (top) and cross-plot of the inversion result at the well location versus the impedance calculated from the well logs (bottom).

References

Diaz, J., P. Weimer, G. Dorn, and R. Bouroullec, 2010, 3D stratigraphic interpretation of Quaternary sediments in the Mensa and Thunder Horse intraslope basins, Mississippi Canyon, northern deep Gulf of Mexico: *Gulf Coast Association of Geological Societies Transactions*, v. 60, p. 191-205.

Hood, K. C., L. M. Wenger, O. P. Gross, and S. C. Harrison, 2002, Hydrocarbon systems analysis of the northern Gulf of Mexico: Delineation of hydrocarbon migration pathways using seeps and seismic imaging, in D. Schumacher and L. A. LeSchack, eds., Surface exploration case histories: Applications of geochemistry, magnetics, and remote sensing: *AAPG Studies in Geology* 48 and *Society of Exploration Geophysicists Geophysical Reference Series 11*, p. 25–40.

Lapinski, T., R. Bouroullec, and P. Weimer, 2004, Structural evolution of the Thunder Horse mini-basin, Mississippi Canyon, northern deep Gulf of Mexico: *GCAGS Transactions,* v. 54, p. 313-326.

Lapinski, T., P. Weimer, and R. Bouroullec, 2004, Sequence stratigraphic evolution of Thunder Horse mini-basin, Mississippi Canyon, northern deep Gulf of Mexico: *GCAGS Transactions*, v. 54, p. 327-341.

McBride, B., M. Rowan, P. Weimer, (1998), The evolution of allochthonous salt systems, northern Green Canyon and Ewing Bank (offshore Louisiana), northern Gulf of Mexico, *AAPG Bulletin*, v. 85, i.5B, p. 1013-1036.

Rowan, M. G. and P. Weimer, 1998: salt-sediment interaction, Northern Green Canyon and Ewing Bank (offshore Louisiana), Northern Gulf of Mexico1, *AAPG Bulletin*, V. 82, No.5B (May1998, part B), p. 1055-1082.

Stover, S.C., P. Weimer, S. Ge, 2001, The effects of allochthonous salt evolution and overpressure development on source rock thermal maturation: a two-dimensional transient study in the northern Gulf of Mexico Basin, *Petroleum Geosciences*, 7, 281-290.

CONSTRAINING BASIN THERMAL HISTORY AND PETROLEUM GENERATION HISTORY USING PALEOCLIMATE DATA IN THE PICEANCE BASIN, COLORADO

Yao Tong[1], Daniel E. Ibarra[2], Jeremy K. Caves[2], Tapan Mukerji[1], and Stephan A. Graham[2]
[1]*Department of Energy Resources Engineering, Stanford University*
[2]*Department of Geological Sciences, Stanford University*

Abstract

Basin thermal history is critical to reconstructing subsidence, uplift, and petroleum generation in sedimentary basins. In this study, we propose a novel approach to constrain basin thermal history using paleoclimate temperature reconstructions. We study the impact of this approach on source rock maturation and hydrocarbon generation in a subaerial sedimentary basin. Paleoclimate data from macroflora assemblages were used to compile mean annual temperature (MAT) for the Piceance Basin. One-dimensional (1-D) basin models were constructed using two different upper thermal boundary condition scenarios. The first used the standard "Auto SWIT" tool of PetroMod software, an algorithm that draws on a generalized database of surface temperatures as a function of latitude and continent through time. The second incorporates paleoclimate data local to the sedimentary basin of interest. Model predictions indicate that source rock maturation is very sensitive to the upper thermal boundary condition. Cumulatively, there is a decrease of 0.26% in predicted vitrinite reflectance, a decrease of 11 % in source rock transformation ratio, and a decrease of 18% in hydrocarbon mass generation using the local temperature data compared to the standard case. This is because the standard data fail to consider the cooling effect of extreme elevations in significantly uplifted basins.

Methodology

The thermal evolution of the source rock in sedimentary basins can be modeled by solving the heat flow equation given upper and lower thermal boundary conditions (Hantschel and Kauerauf, 2009). The upper thermal boundary condition is estimated from the sediment-water-interface temperature (Hantschel & Kauerauf, 2009). This temperature profile contains two parts: the past temperature and the present-day surface temperature. For the estimate of paleo sediment-water-interface temperature, an average paleo-air-surface temperature (TS) is first estimated from paleolatitude (Wygrala, 1989), which requires knowledge of the paleolatitude of the study area. Then, TS is corrected to the actual sediment-water-interface temperature (TSWI) accounting for the paleowater depth. This TSWI served as the upper thermal boundary condition in the past. For the estimation of modern temperature, the annual mean ground surface temperature is often obtained from mean air temperature (www.worldclimate.com) using the present-day latitude of the study area, and water depth is accounted for following the equations from Beardsmore and Cull (2001) and Hantschel and Kauerauf (2009).

These methods provide a basis for estimating upper thermal boundary temperatures and they are especially suitable for marine basins with known paleowater depths. One limitation of these methods is a poor estimation of surface temperatures in terrestrial basins, which are subaerially exposed and generally experienced more complex temperature variations relative to the stable depositional environment of many marine basins.

In order to better quantify basin thermal history in a subaerial setting, we propose a new method to estimate the upper thermal boundary conditions using paleoclimate data in the Piceance Basin, Colorado. Paleobotanical data are used to quantify changes in the regional MAT in the study area. Two primary approaches have been used to estimate paleotemperatures using macroflora: Leaf Margin Analysis (LMA) (Wilf, 1997) and Climate-Leaf Analysis Multivariate Program (CLAMP) (Wolfe, 1995). We compiled all available temperature estimates from Colorado, Utah, Nevada and Wyoming (Figure 1). The inclusion of estimates from Nevada is necessary to provide paleotemperature estimates during the Miocene, in particular during the mid-Miocene, a period of known global warmth relative to the Oligocene and late Neogene. The resulting temperature compilation suggests temperatures of 17 to 25°C during the Eocene, which drop through the Cenozoic to modern temperatures of 5 to 12°C. This trend corresponds well to both timing of uplift of the Piceance Basin (Mix et al., 2011; Smith et al., 2014) and global cooling and pCO_2 decreases (Zachos et al., 2001; Beerling and Royer, 2011) from the Late Cretaceous to the Neogene.

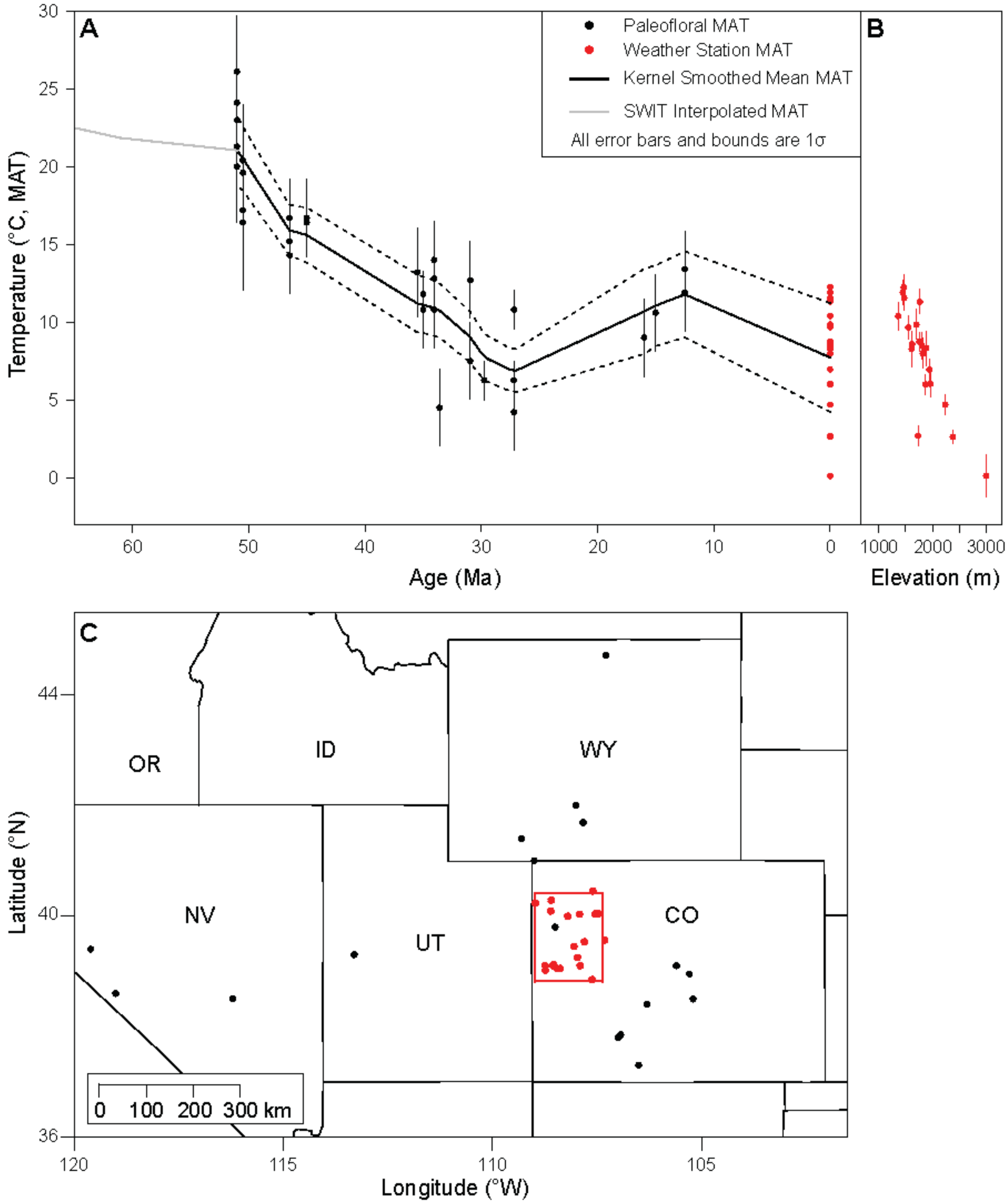

Figure 1. The upper chart shows the compiled Mean Annual Surface Temperature for the Piceance Basin using paleobotanical data (black curve is the MAT estimations, black dots are data points used, red dots are MAT measurements from present-day weather stations). The lower chart shows the paleobotanical data locations (black dots) and the modern weather station locations (red dots)

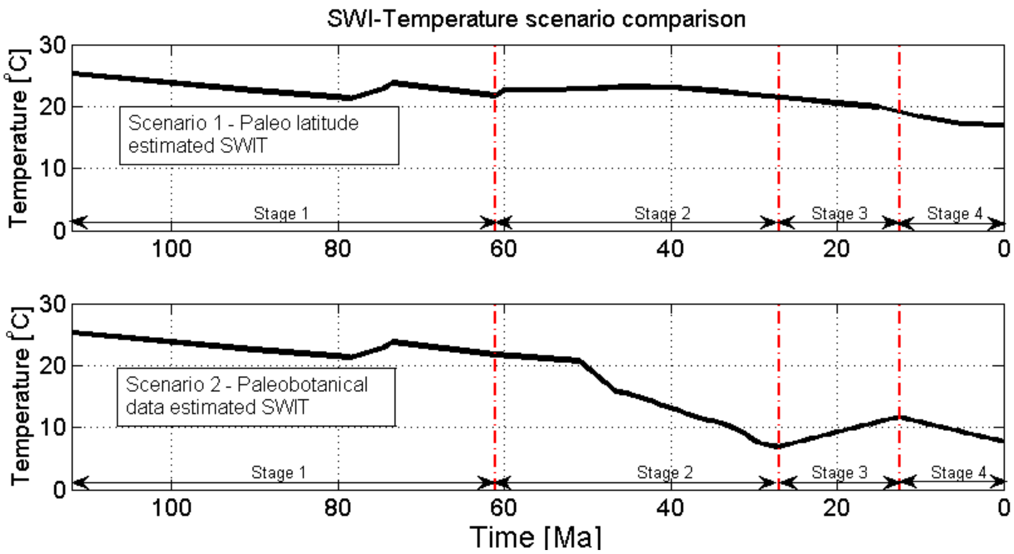

Figure 2. Comparison of two different surface temperature profiles. The upper chart shows the first SWIT scenario, which we estimate using the globally-averaged, latitudinal-dependent temperature reconstructions from Wygrala (1989). The lower chart shows the second SWIT scenario, which we construct by integrated paleobotanical temperature data.

Basin model and results

In order to evaluate different thermal boundary conditions and isolate their impact, we construct two basin models using two different surface temperature profiles, leaving all other model inputs unchanged. The basin models were constructed for the Exxon Love Ranch 1 well using 1-D basin modeling program (PetroMod 1D). We selected this well because (1) it is located in the northern central part of the basin where the source rock burial history is well known and (2) abundant geologic and geochemical data are available from previous studies (Yurewicz et al., 2003, 2008; Zhang et al., 2008). Model scenario one uses the SWIT profile of Wygrala (1989) and model scenario two uses the SWIT profile compiled from local and regional paleoclimate data (Figure 2).

The impact of the upper thermal boundary condition on the predictions of source rock maturity, transformation ratio, and hydrocarbon generation are shown in Figure 3.

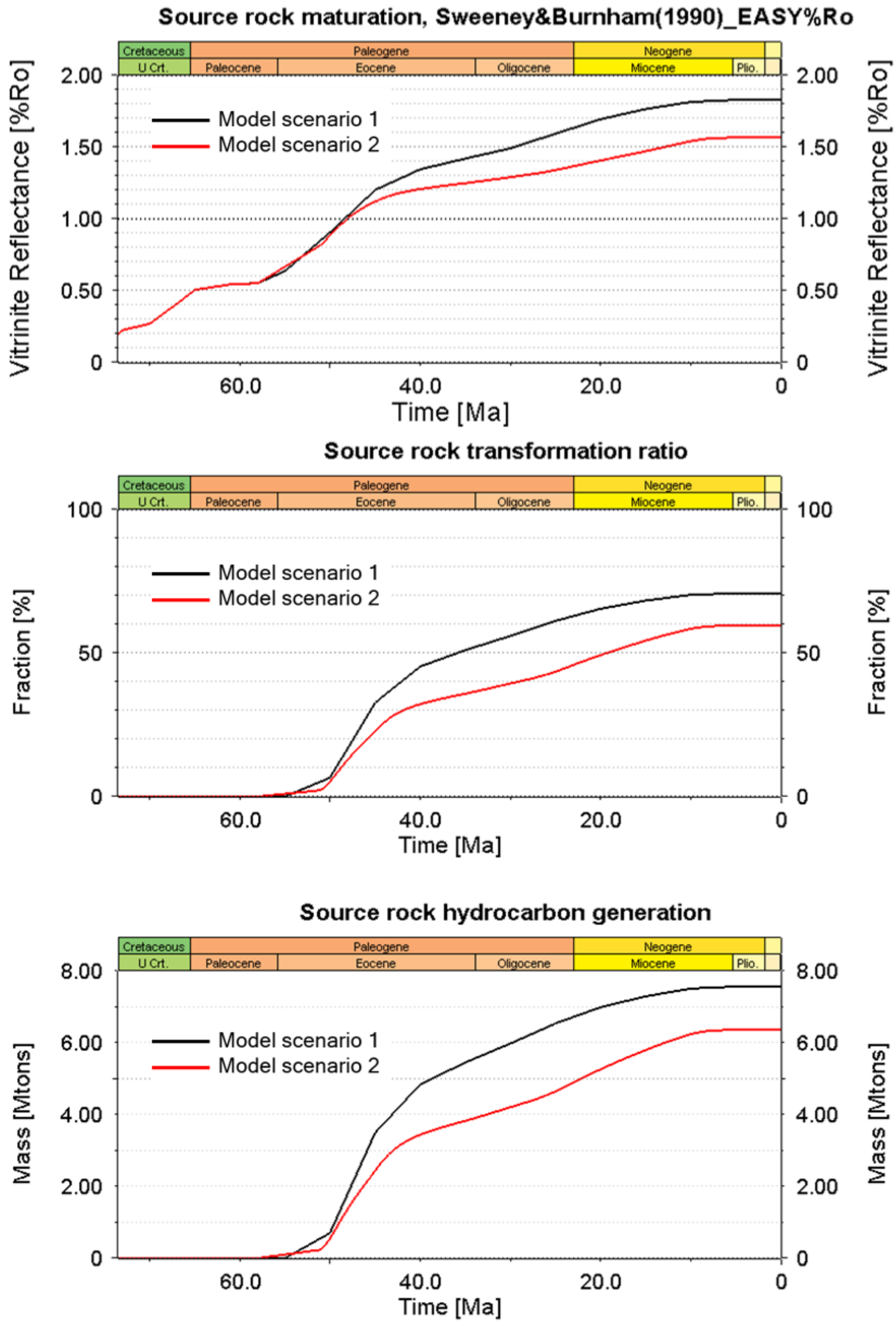

Figure 3. Model comparisons of source rock maturation, source rock transformation ratio, and hydrocarbon generation mass. Black curves are predictions from model scenario one (Auto SWIT tool) and red curves are predictions from model scenario two (local paleoclimate data).

For the source rock maturation predictions, both models show gradually increasing maturity resulting from continuously depositing overburden sediment until the latest Cenozoic. However, the maturation rates over time show different behavior. From the Late Cretaceous until the early-mid Eocene, both models show similar maturation patterns; however, from that point on, the maturation prediction from scenario 2 diverges from scenario 1 and remains nearly parallel but lower in magnitude. This observation closely corresponds to the steep temperature decrease in scenario 2, as the paleobotanical data indicate a colder surface temperature resulting from uplift after the early-mid Eocene. For the maturation prediction from scenario two, there is a pronounced slope change from mid-Oligocene to mid-Miocene. Overall, we observe that source rock maturation predictions are sensitive to the choice of SWIT history. The local temperature variations captured by paleobotanical data provide extra information to constrain basin thermal history.

The source rock transformation ratio and hydrocarbon generation predictions show a similar evolution over time. The source rock transformation ratio is defined as the fraction of source rock that has been thermally matured and generated hydrocarbon; when this fraction of matured source rock increases, we expect greater generation of hydrocarbons from the source rock. Comparing between the model scenarios, the slope changes given by the second model scenario are noteworthy. For instance, model scenario two (red curve) shows a slope change in source rock transformation ratio prediction around 25 Ma, indicating that the source rock transformation ratio sharply increased in the Oligocene. This corresponds well with the upper thermal boundary condition change in SWIT scenario two, the increase of SWIT during stage 3 (Figure 6). The overall fraction of matured source rock and hydrocarbon generation increases cumulatively. However, the evolution through time differs, indicating that the source rock "cooking process" is significantly different. In the late Oligocene, scenario 1 predicts a 60% transformation ratio as compared to only 40% as predicted by scenario 2. Assuming the same hydrocarbon trap mechanism, the charge potential would be quite different at a given point in time. Also, the resulting peak hydrocarbon generation time (i.e., the "critical moment") will change accordingly. As this timing factor is crucial to determine whether the hydrocarbon charge is favorable for petroleum accumulation or not, constraining the uncertainties in the thermal conditions will ultimately reduce the petroleum exploration risk.

Summary and Conclusions

Results from two basin model scenarios for the Piceance Basin show that the simulated source rock maturation, transformation ratio and hydrocarbon generation varies significantly given different SWIT conditions. In and of itself this is not surprising, but our results underscore the importance of correctly capturing surface thermal history in subaerial basins where elevation changes occur over time. The differences shown in the model prediction represent the uncertainties given by different upper thermal boundary conditions. These uncertainties could be reduced using our proposed approach, where terrestrial paleoclimate data are utilized to more accurately pinpoint basin thermal history. The methodology is generally applicable for any terrestrial setting basin with reliable paleoclimate data. Presumably, the effects demonstrated here would be much more pronounced in basins where surface elevation changes are even more substantial, such as basins of the Tibet Plateau, where elevation changed from sea level to up to 5-6 kilometers from Cretaceous to Cenozoic time (Ritts et al., 2008; Wang et al., 2008, 2014).

References

Beardsmore, G. R., and J. P. Cull, 2001, Crustal Heat Flow. *A Guide to Measurement and Modelling*: Cambridge University Press.

Beerling, D. J., and D. L. Royer, 2011, Convergent Cenozoic CO2 history: *Nature Geoscience*, v. 4, no. 7, p. 418–420, doi:10.1038/ngeo1186.

Hantschel, T., and A. I. Kauerauf, 2009, *Fundamentals of basin and petroleum systems modeling, in Fundamentals of Basin and Petroleum Systems Modeling*: p. 1–476, doi:10.1007/978-3-540-72318-9.

Mix, H. T., A. Mulch, M. L. Kent-Corson, and C. P. Chamberlain, 2011, Cenozoic migration of topography in the North American Cordillera: *Geology*, v. 39, p. 87–90, doi:10.1130/G31450.1.

Ritts, B. D., Y. Yue, S. A. Graham, E. R. Sobel, O. A. Abbink, and D. Stockli, 2008, From sea level to high elevation in 15 million years: Uplift history of the northern Tibetan Plateau margin in the Altun Shan: *American Journal of Science*, v. 308, no. 5, p. 657–678.

Smith, M. E., A. R. Carroll, B. R. Jicha, E. J. Cassel, and J. J. Scott, 2014, Paleogeographic record of Eocene Farallon slab rollback beneath western North America: *Geology*, v. 42, no. 12, p. 1039–1042.

Wang, C., J. Dai, X. Zhao, Y. Li, S. A. Graham, D. He, B. Ran, and J. Meng, 2014, Outward-growth of the Tibetan Plateau during the Cenozoic: A review: *Tectonophysics*, v. 621, p. 1–43.

Wang, C., X. Zhao, Z. Liu, P. C. Lippert, S. A. Graham, R. S. Coe, H. Yi, L. Zhu, S. Liu, and Y. Li, 2008, Constraints on the early uplift history of the Tibetan Plateau: *Proceedings of the National Academy of Sciences*, v. 105, no. 13, p. 4987–4992.

Wilf, P., 1997, When are leaves good thermometers? A new case for leaf margin analysis: P*aleobiology*, v. 23, no. 3, p. 373–390.

Wolfe, J. A., 1995, Paleoclimatic estimates from Tertiary leaf assemblages: *Annual Review of Earth and Planetary Sciences*, v. 23, p. 119–142.

Wygrala, B. P., 1989, Integrated study of an oil field in the southern Po Basin Northern Italy: University of Cologne.

Yurewicz, D. A., K. M. Bohacs, J. D. Yeakel, and K. Kronmueller, 2003, Source Rock Analysis and Hydrocarbon Generation, Mesaverde Group and Mancos Shale, Northern Piceance Basin, Colorado, in *Piceance Basin Guidebook*: p. 130–153.

Yurewicz, D. A., J. Kendall, K. Kronmueller, T. C. Ryan, K. M. Bohacs, R. E. Klimentidis, M. E. Meurer, and J. D. Yeakel, 2008, Controls on Gas and Water Distribution, Mesaverde Basin-centered Gas Play, Piceance Basin, Colorado, in S. P. Cumella, K. W. Shanley, and W. K. Camp, eds., Understanding, exploring, and developing tight-gas sands—2005 Vail Hedberg Conference: *AAPG Hedberg Series*: p. 105–136, doi:10.1306/13131053H31639.

Zachos, J., M. Pagani, L. Sloan, E. Thomas, and K. Billups, 2001, Trends, rhythms, and aberrations in global climate 65 Ma to present: *Science*, v. 292, no. 5517, p. 686–693.

Zhang, E., R. J. Hill, B. J. Katz, and Y. Tang, 2008, Modeling of gas generation from the Cameo coal zone in the Piceance Basin, Colorado: *AAPG Bulletin*, v. 92, no. 8, p. 1077–1106, doi:10.1306/04020806015.